Molecular Baskets form Inclusion Complexes with Phenethylamine Drugs in Water

Tyler J. Finnegan,[a] Christopher Mortensen,[a] Jovica D. Badjić[a]*

[a] T. J. Finnegan, C. Mortensen and Prof. J. D. Badjić
Department of Chemistry and Biochemistry
The Ohio State University
100 West 18th Avenue, Columbus, Ohio 43210 (USA)
E-mail: badjic.1@osu.edu
100 West 18th Avenue, Columbus, Ohio 43210 (USA)

Supporting Information

General information:

All chemicals were purchased from commercial sources and used as received. All titrations were performed using 90% 30 mM phosphate buffer solution with 10% D_2O, pH = 7.0 ± 0.1 as the solvent. ^1H NMR spectra were recorded at 300 K by a Bruker 600 MHz spectrometer. Dimethylformamide solvent peaks were used as internal standard to calibrate chemical shift. Deuterated solvents D_2O were purchased from Cambridge Isotope Laboratories. High resolution mass spectrometry electrospray ionization (HRMS-ESI) spectra were recorded on a Bruker Micro-TOF ESI instrument using 25 mM ammonium bicarbonate in water, pH = 7.0 ± 0.1 as the solvent.

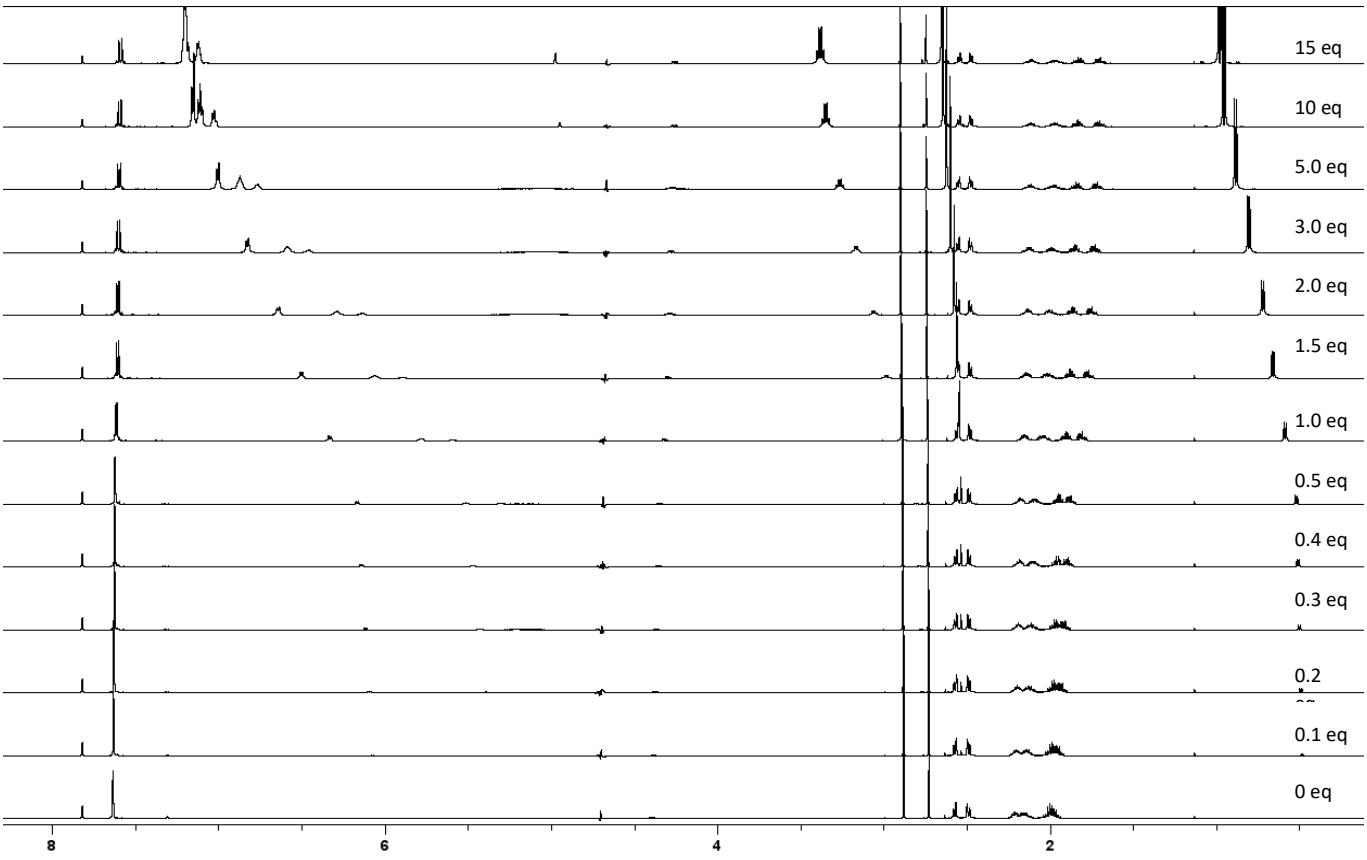

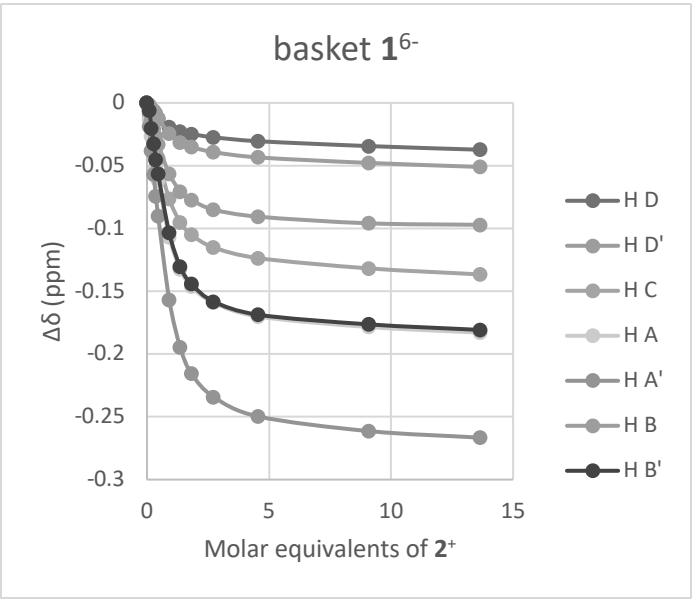

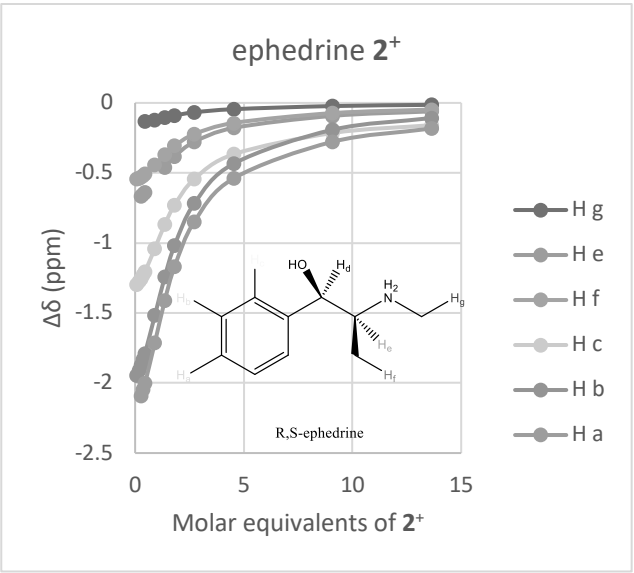

Figure S1. (Top) ^{1}H NMR spectra (600 MHz, 300K) of 1.0 mM solution of basket **1** (i.e., $\mathbf{1}^{6-}$), in 30 mM phosphate buffer solution at pH = 7.0 ± 0.1 and containing 10% D_2O, obtained after incremental addition of 60.0 mM standard solution of (1*R*, 2*S*)-ephedrine $\mathbf{2}^{+}$; note that molar equivalents of guest $\mathbf{2}^{+}$ are shown on right. (Bottom) Magnetic perturbation ($\Delta\delta = \delta_{observed} - \delta_{free}$) of resonances from basket $\mathbf{1}^{6-}$ (left) and ephedrine $\mathbf{2}^{+}$ (right) obtained in supramolecular titration described on top. Note that we completed three titrations of which only one is shown here.

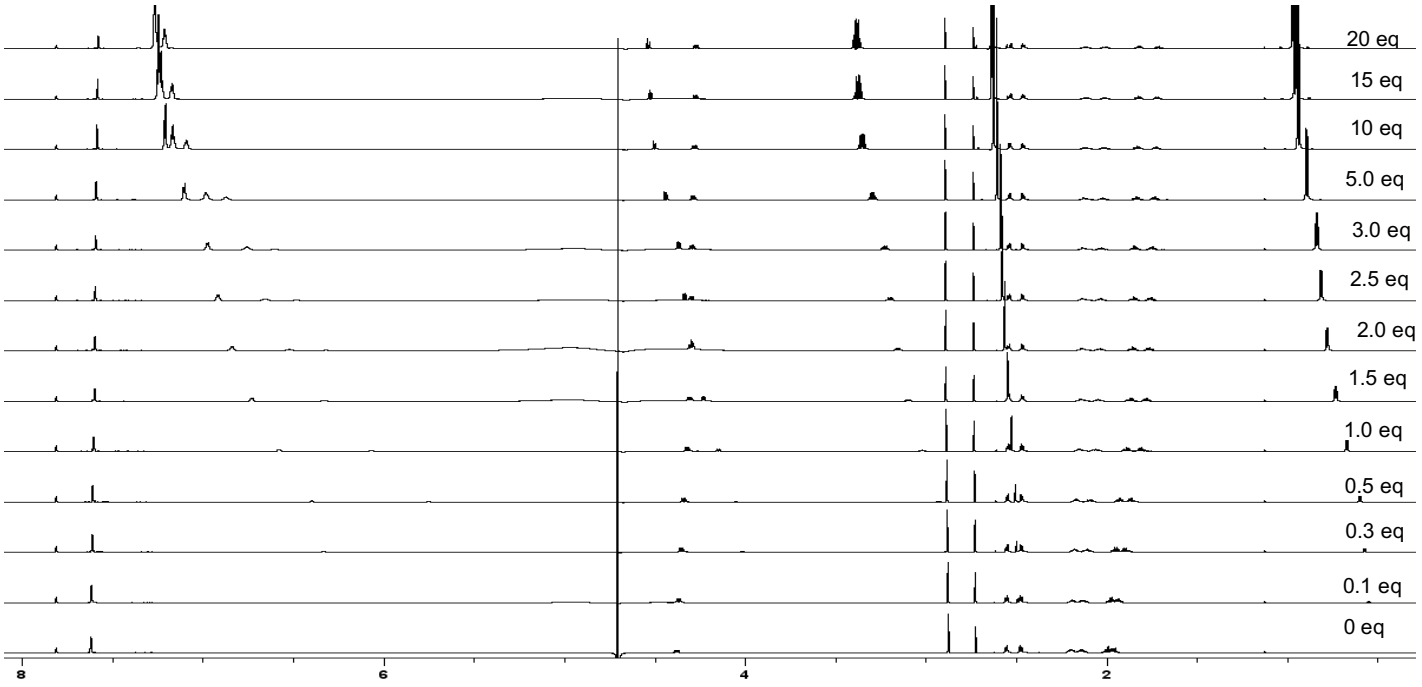

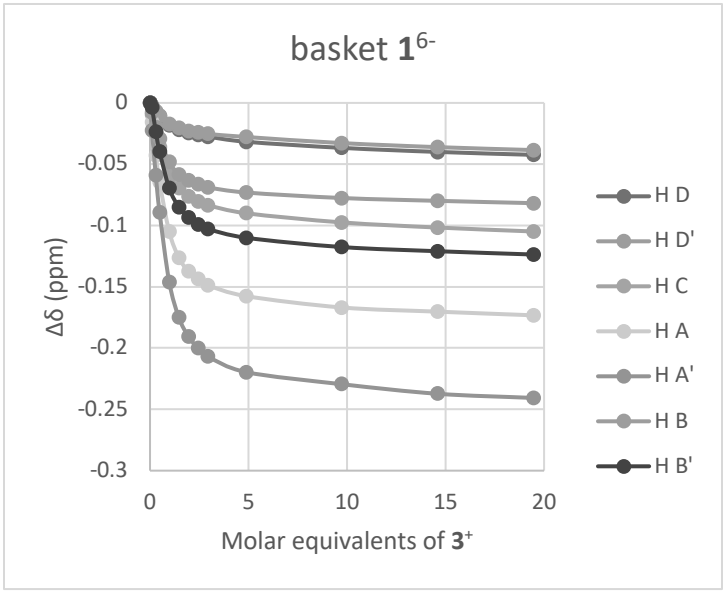

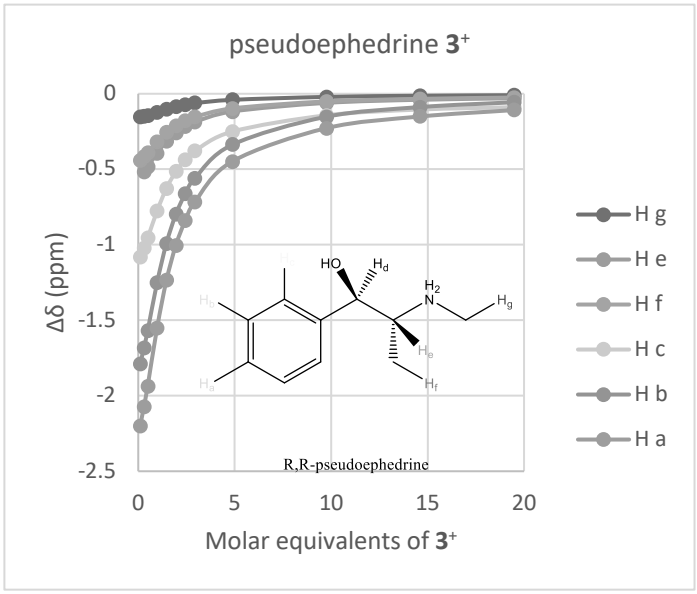

Figure S2. (Top) ^{1}H NMR spectra (600 MHz, 300K) of 1.0 mM solution of basket **1** (i.e., $\mathbf{1}^{6-}$), in 30 mM phosphate buffer solution at pH = 7.0 ± 0.1 and containing 10% D_2O, obtained after incremental addition of 60.0 mM standard solution of (1*R*, 2*R*)-pseudoephedrine $\mathbf{3}^+$; note that molar equivalents of guest $\mathbf{3}^+$ are shown on right. (Bottom) Magnetic perturbation ($\Delta\delta = \delta_{observed} - \delta_{free}$) of resonances from basket $\mathbf{1}^{6-}$ (left) and pseudoephedrine $\mathbf{3}^+$ (right) obtained in supramolecular titration described on top. Note that we completed three titrations of which only one is shown here.

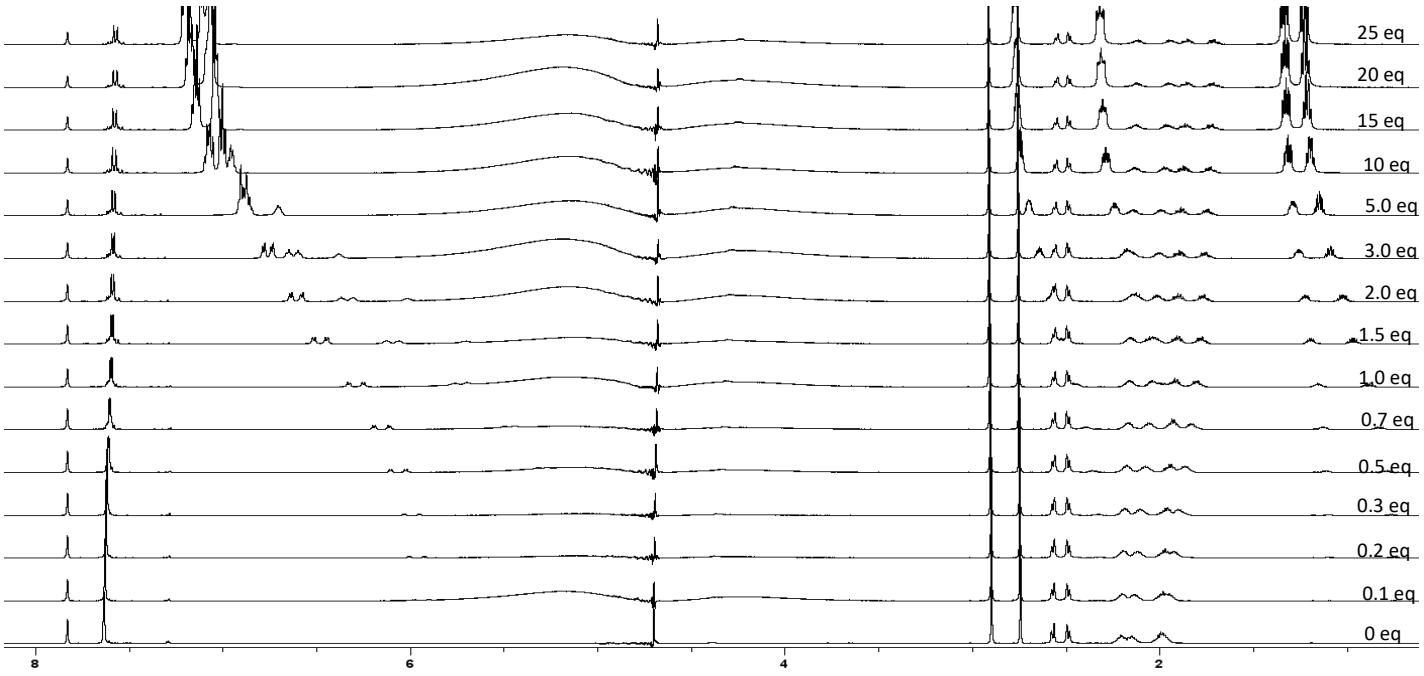

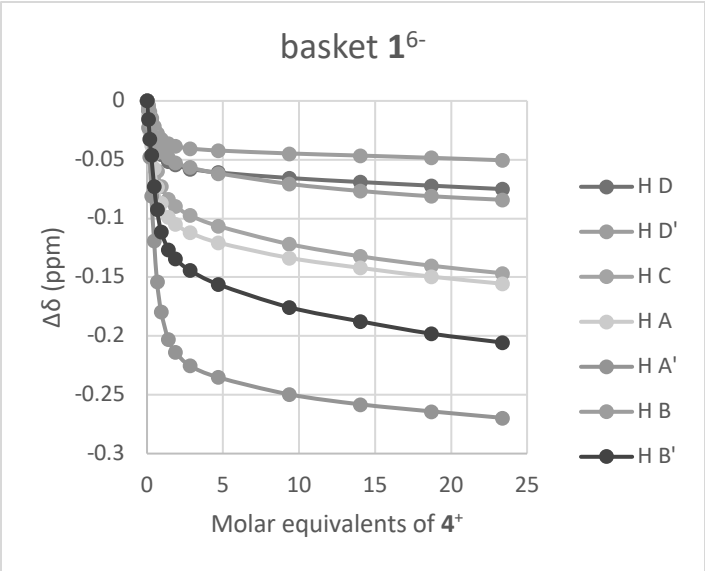

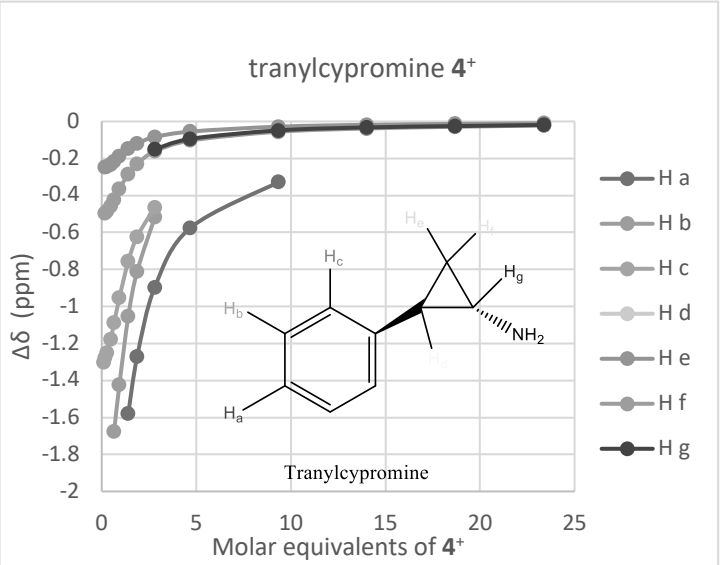

Figure S3. (Top) ^{1}H NMR spectra (600 MHz, 300K) of 1.0 mM solution of basket **1** (i.e., $\mathbf{1}^{6-}$), in 30 mM phosphate buffer solution at pH = 7.0 ± 0.1 and containing 10% D_2O, obtained after incremental addition of 60.0 mM standard solution of (1*S*, 2*R*)-tranylcypromine $\mathbf{4}^{+}$; note that molar equivalents of guest $\mathbf{4}^{+}$ are shown on right. (Bottom) Magnetic perturbation ($\Delta\delta = \delta_{observed} - \delta_{free}$) of resonances from basket $\mathbf{1}^{6-}$ (left) and tranylcypromine $\mathbf{4}^{+}$ (right) obtained in supramolecular titration described on top. Note that we completed three titrations of which only one is shown here.

bindfit FITTER SEARCH BACK TO SUPRAMOLECULAR HOME

Data Browser Picker Pager

Results per page: 7 Jump: 1

Fitter: NMR 1:1 Fit Summary Save

Details

Time to fit	0.3823 s
SSR	2.4167e-4
Fitted datapoints	91
Fitted params	15

Parameters

Parameter (bounds)	Optimised	Error	Initial
K (0 → ∞)	3516.73 M^{-1}	± 2.7403 %	100.00 M^{-1}

Back Next

Welcome! BindFit is currently under development. Although we do our best to test everything, you may occasionally find features that aren't working quite right. Feel free to email us at bugs@opendatafit.org to report anything broken, or suggest any new features you'd like implemented.

Fits Molefractions Details

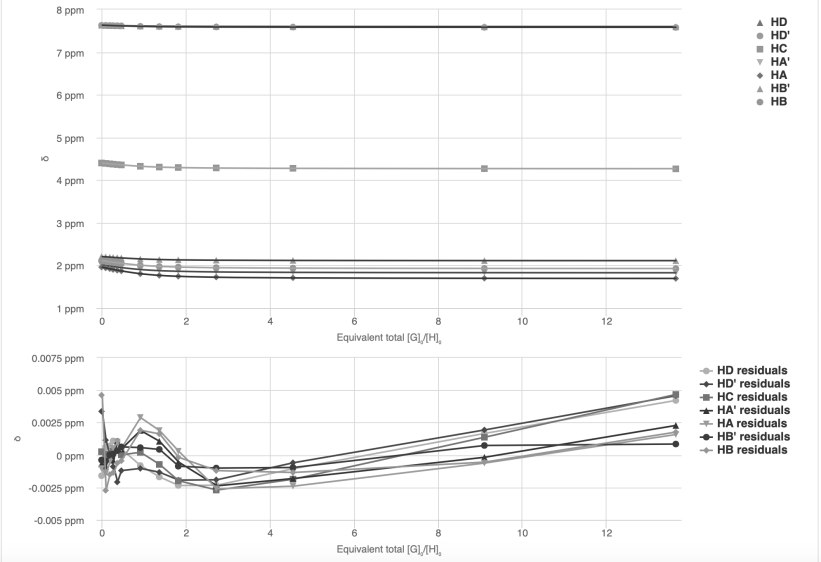

bindfit FITTER SEARCH BACK TO SUPRAMOLECULAR HOME

Data Browser Picker Pager

Results per page: 7 Jump: 1

Fitter: NMR 1:2 Fit Summary Save

Details

Time to fit	1.0748 s
SSR	6.6251e-5
Fitted datapoints	91
Fitted params	23

Parameters

Parameter (bounds)	Optimised	Error	Initial
K_{11} (0 → ∞)	5260.73 M^{-1}	± 2.0780 %	1000.00 M^{-1}
K_{12} (0 → ∞)	66.40 M^{-1}	± 6.4183 %	100.00 M^{-1}

Back Next

Welcome! BindFit is currently under development. Although we do our best to test everything, you may occasionally find features that

Fits Molefractions Details

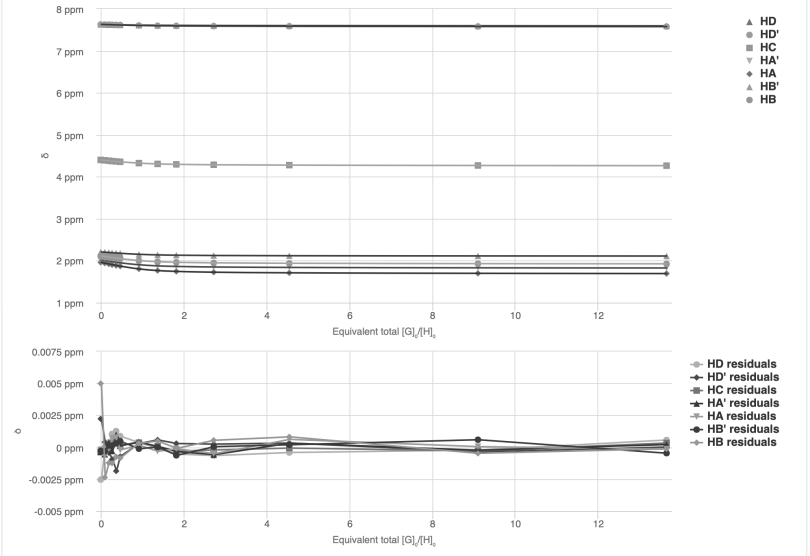

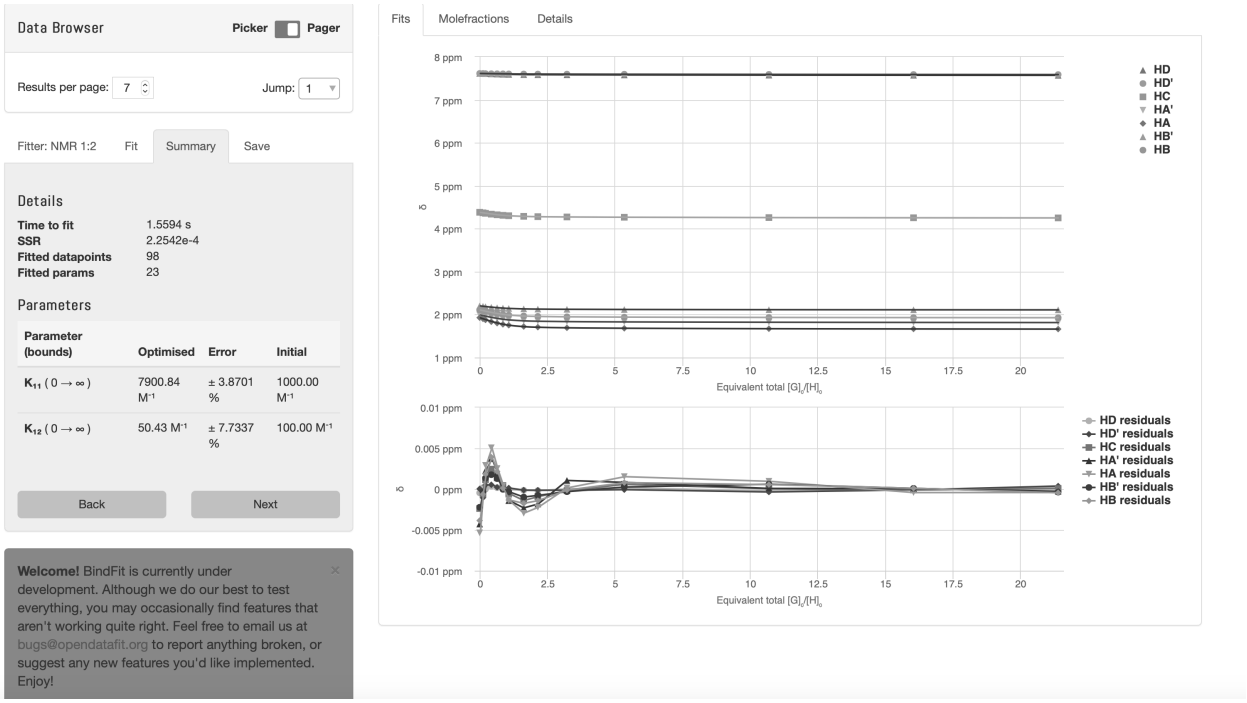

Figure S4. A change in ^{1}H NMR chemical shift of seven resonances from basket $\mathbf{1}^{6-}$ as a function of increasing concentration of ephedrine $\mathbf{2}^{+}$ (Figure S1) were subjected to nonlinear regression analysis using 1:1 (top), 1:2 (middle), and 2:1 (bottom) binding models; see: supramolecular.org for more information about these models and fitting procedures. Covariance of fits were 5.5371 · 10^{-4} (1:1), 1.5179 · 10^{-4} (1:2), and 2.6449 · 10^{-4} (2:1). Note that for two additional titrations covariances were found to be: Titration 2 = 1.4517 · 10^{-3} (1:1), 2.6825 · 10^{-4} (1:2), and 3.9438 · 10^{-4} (2:1); Titration 3 = 1.6308 · 10^{-3} (1:1), 4.5012 · 10^{-4} (1:2), and 3.2895 · 10^{-4} (2:1). For 1:2 binding model, we obtained the following values for binding constants: Titration 1 – K_1 = 5261 M^{-1} and K_2 = 66 M^{-1}; Titration 2 – K_1 = 7815 M^{-1} and K_2 = 45 M^{-1}; Titration 3 – K_1 = 7900 M^{-1} and K_2 = 50 M^{-1}. All data files are available from the corresponding author for further analysis. Please use badjic.1@osu.edu for submitting your request.

bindfit FITTER SEARCH BACK TO SUPRAMOLECULAR HOME

Data Browser Picker Pager

Results per page: 7 Jump: 1

Fitter: NMR 1:1 Fit Summary Save

Details

Time to fit	0.2742 s
SSR	7.1417e-4
Fitted datapoints	91
Fitted params	15

Parameters

Parameter (bounds)	Optimised	Error	Initial
K (0 → ∞)	3175.65 M^{-1}	± 5.1468 %	100.00 M^{-1}

Back Next

Welcome! BindFit is currently under development. Although we do our best to test everything, you may occasionally find features that aren't working quite right. Feel free to email us at bugs@opendatafit.org to report anything broken, or suggest any new features you'd like implemented.

Fits Molefractions Details

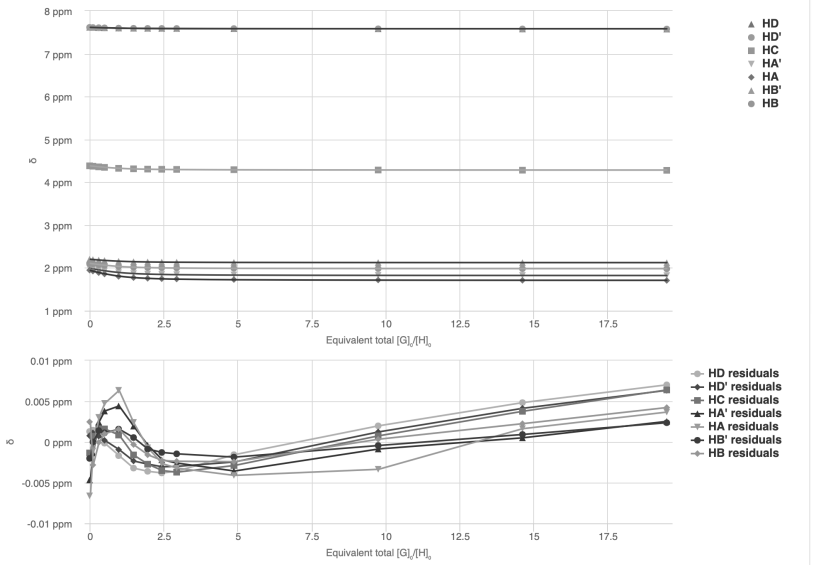

Data Browser Picker Pager

Results per page: 7 Jump: 1

Fitter: NMR 1:2 Fit Summary Save

Details

Time to fit	1.4945 s
SSR	1.1167e-4
Fitted datapoints	91
Fitted params	23

Parameters

Parameter (bounds)	Optimised	Error	Initial
K_{11} (0 → ∞)	6329.50 M^{-1}	± 3.5188 %	1000.00 M^{-1}
K_{12} (0 → ∞)	51.42 M^{-1}	± 5.3599 %	100.00 M^{-1}

Back Next

Welcome! BindFit is currently under development. Although we do our best to test everything, you may occasionally find features that aren't working quite right. Feel free to email us at

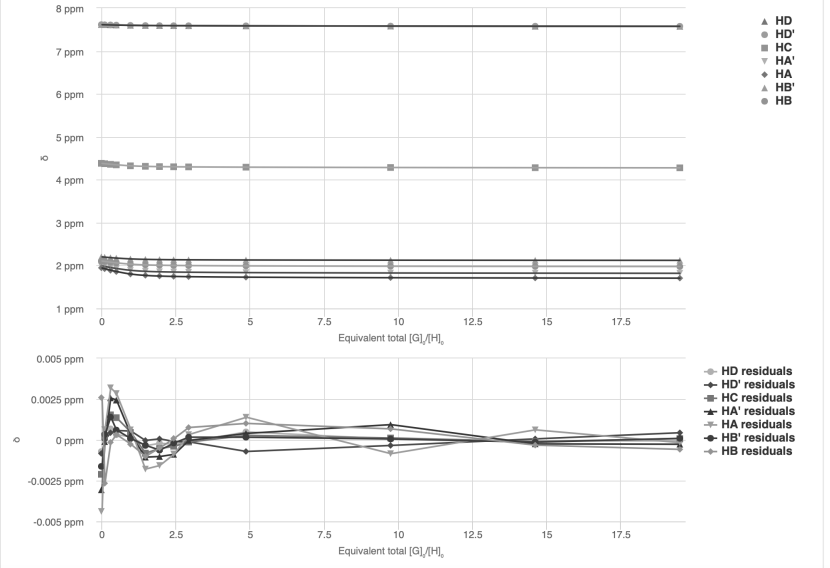

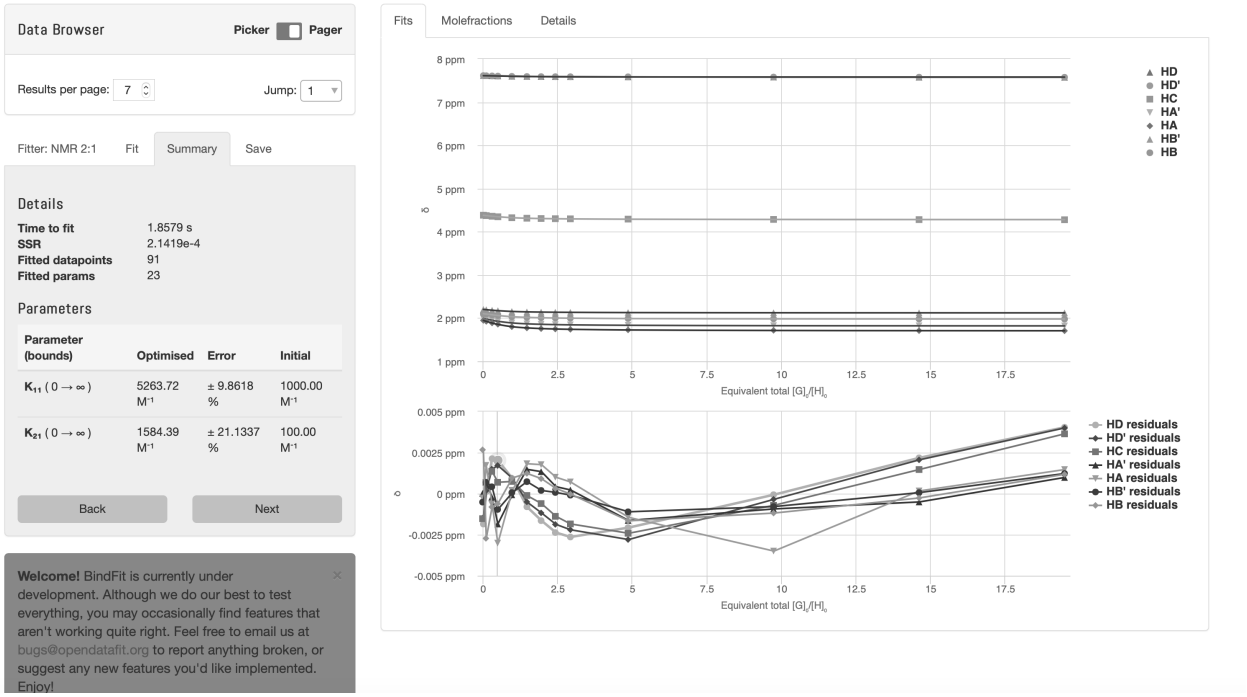

Figure S5. A change in ^{1}H NMR chemical shift of seven resonances from basket $\mathbf{1}^{6-}$ as a function of increasing concentration of pseudoephedrine $\mathbf{3}^{+}$ (Figure S2) were subjected to nonlinear regression analysis using 1:1 (top), 1:2 (middle), and 2:1 (bottom) binding models; see: supramolecular.org for more information about these models and fitting procedures. Covariance of fits were 1.9522 $\cdot 10^{-3}$ (1:1), 3.0535 $\cdot 10^{-4}$ (1:2), and 5.8550 $\cdot 10^{-4}$ (2:1). Note that for two additional titrations covariances were found to be: Titration 2 = 2.2833 $\cdot 10^{-3}$ (1:1), 5.1843 $\cdot 10^{-4}$ (1:2), and 5.4900 $\cdot 10^{-4}$ (2:1); Titration 3 = 2.4308 $\cdot 10^{-3}$ (1:1), 1.1997 $\cdot 10^{-3}$ (1:2), and 8.0538 $\cdot 10^{-5}$ (2:1). For 1:2 binding model, we obtained the following values for binding constants: Titration 1 – K_1 = 6329 M^{-1} and K_2 = 51 M^{-1}; Titration 2 – K_1 = 7864 M^{-1} and K_2 = 52 M^{-1}; Titration 3 – K_1 = 4631 M^{-1} and K_2 = 72 M^{-1}. All data files are available from the corresponding author for further analysis. Please use badjic.1@osu.edu for submitting your request.

bindfit FITTER SEARCH BACK TO SUPRAMOLECULAR

Data Browser Picker Pager

Results per page: 5 Jump: 1

Fitter: NMR 1:1 Fit Summary Save

Details

Time to fit	0.2794 s
SSR	7.3120e-3
Fitted datapoints	105
Fitted params	15

Parameters

Parameter (bounds)	Optimised	Error	Initial
K (0 → ∞)	3452.54 M^{-1}	± 14.2702 %	100.00 M^{-1}

Back Next

Welcome! BindFit is currently under development. Although we do our best to test everything, you may occasionally find features that aren't working quite right. Feel free to email us at bugs@opendatafit.org to report anything broken, or suggest any new features you'd like implemented. Enjoy!

Fits Molefractions Details

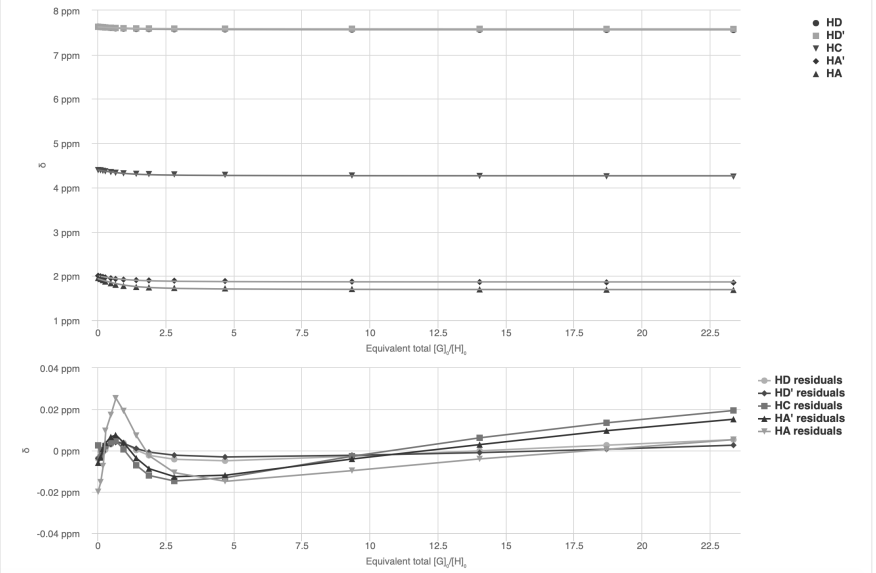

bindfit FITTER SEARCH BACK TO SUPRAMOLECULAR HOME

Data Browser Picker Pager

Results per page: 7 Jump: 1

Fitter: NMR 1:2 Fit Summary Save

Details

Time to fit	1.5902 s
SSR	1.4549e-3
Fitted datapoints	105
Fitted params	23

Parameters

Parameter (bounds)	Optimised	Error	Initial
K_{11} (0 → ∞)	32056.51 M^{-1}	± 27.4670 %	1000.00 M^{-1}
K_{12} (0 → ∞)	25.33 M^{-1}	± 5.8183 %	100.00 M^{-1}

Back Next

Welcome! BindFit is currently under development. Although we do our best to test everything, you may occasionally find features that aren't working quite right. Feel free to email us at

Fits Molefractions Details

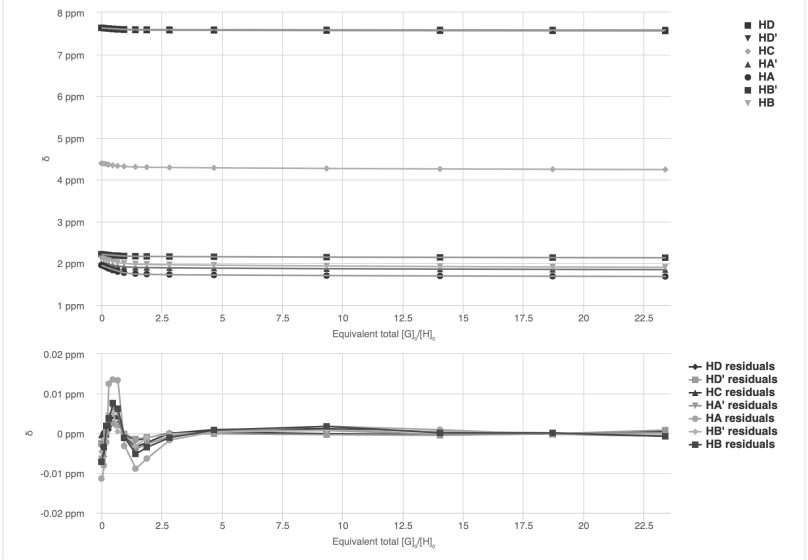

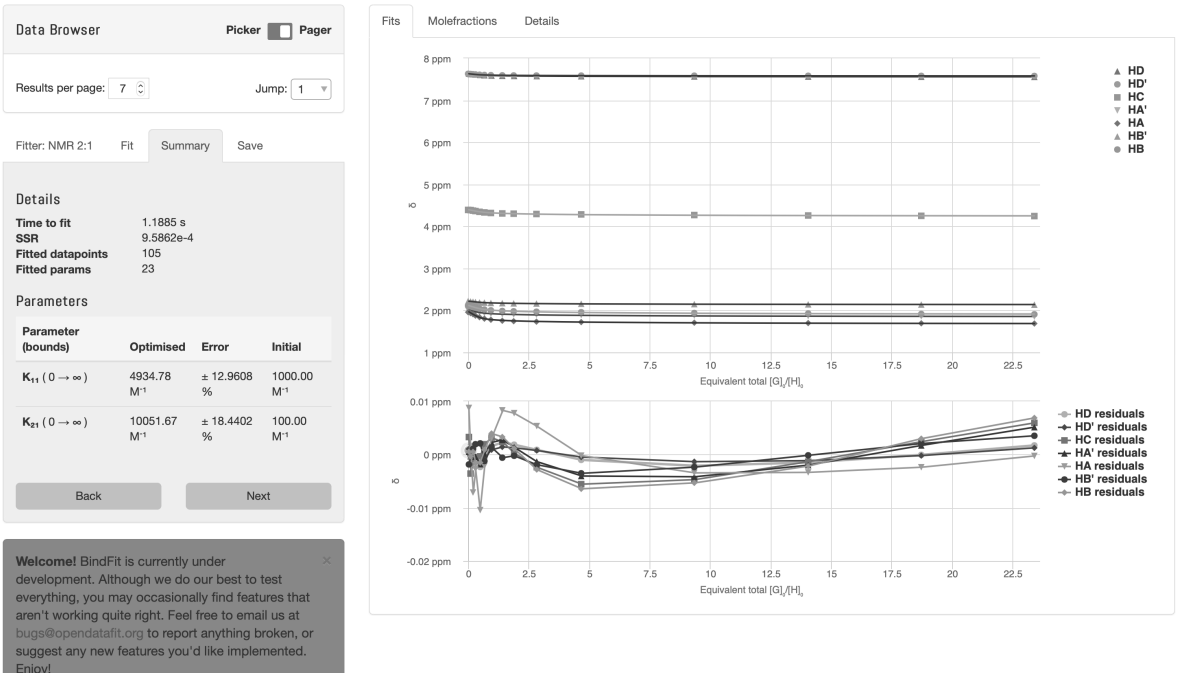

Figure S6. A change in ^{1}H NMR chemical shift of seven resonances from basket $\mathbf{1}^{6-}$ as a function of increasing concentration of tranylcypromine $\mathbf{4}^{+}$ (Figure S3) were subjected to nonlinear regression analysis using 1:1 (top), 1:2 (middle), and 2:1 (bottom) binding models; see: supramolecular.org for more information about these models and fitting procedures. Covariance of fits were $1.5076 \cdot 10^{-2}$ (1:1), $2.9997 \cdot 10^{-3}$ (1:2), and $1.9764 \cdot 10^{-3}$ (2:1). Note that for two additional titrations covariances were found to be: Titration 2 = $8.1079 \cdot 10^{-3}$ (1:1), $5.5525 \cdot 10^{-4}$ (1:2), and $2.2728 \cdot 10^{-3}$ (2:1); Titration 3 = $1.1419 \cdot 10^{-2}$ (1:1), $1.3002 \cdot 10^{-3}$ (1:2), and $2.3828 \cdot 10^{-3}$ (2:1). For 1:2 binding model, we obtained the following values for binding constants: Titration 1 – K_1 = 32056 M^{-1} and K_2 = 25 M^{-1}; Titration 2 – K_1 = 10099 M^{-1} and K_2 = 37 M^{-1}; Titration 3 – K_1 = 19451 M^{-1} and K_2 = 54 M^{-1}. All data files are available from the corresponding author for further analysis. Please use badjic.1@osu.edu for submitting your request.

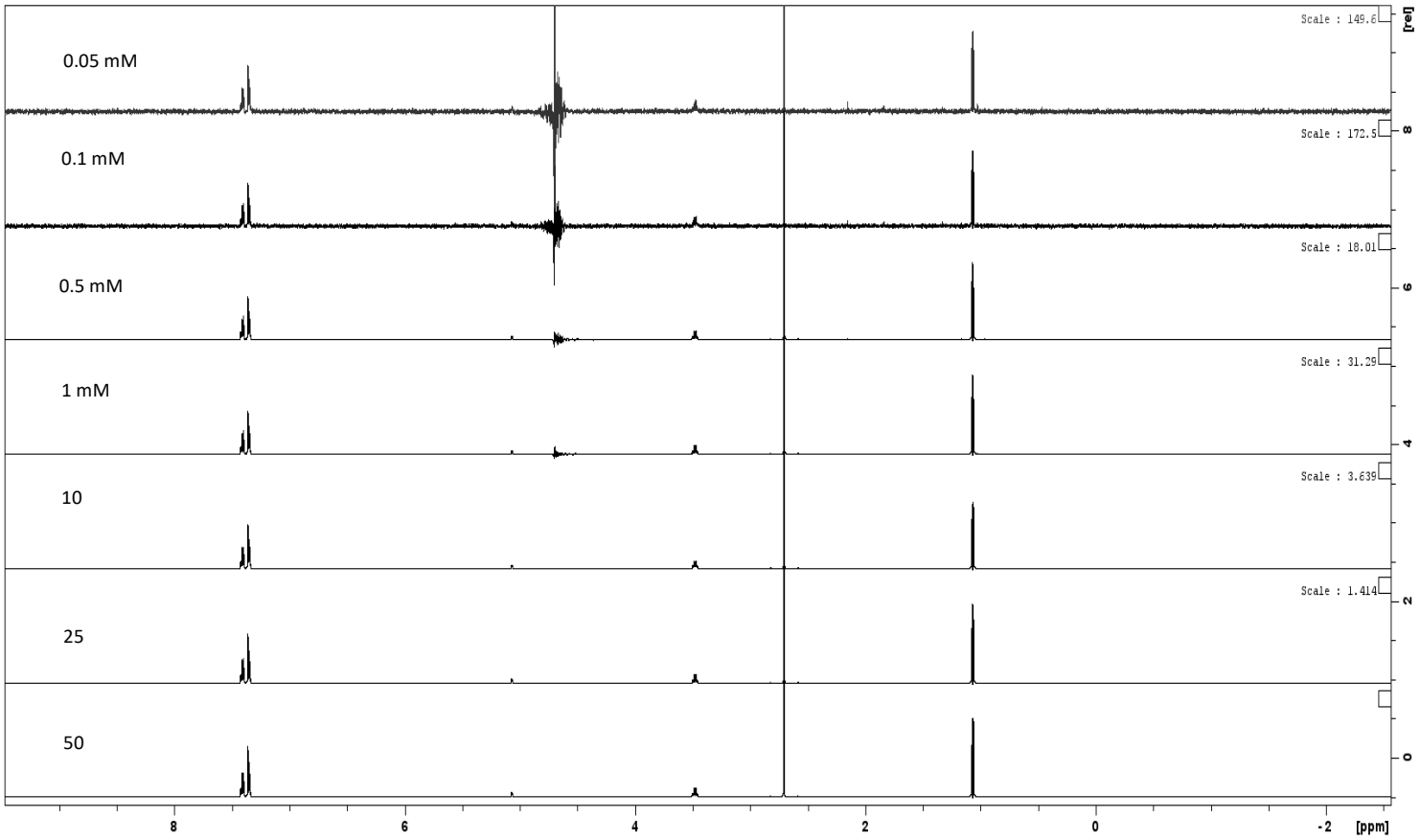

Figure S7. ^{1}H NMR (600 MHz, 298 K) spectra of 0.05 to 50 mM ephedrine $\mathbf{2}^{+}$ in 30 mM phosphate buffer solution at pH 7.0 ± 0.1.

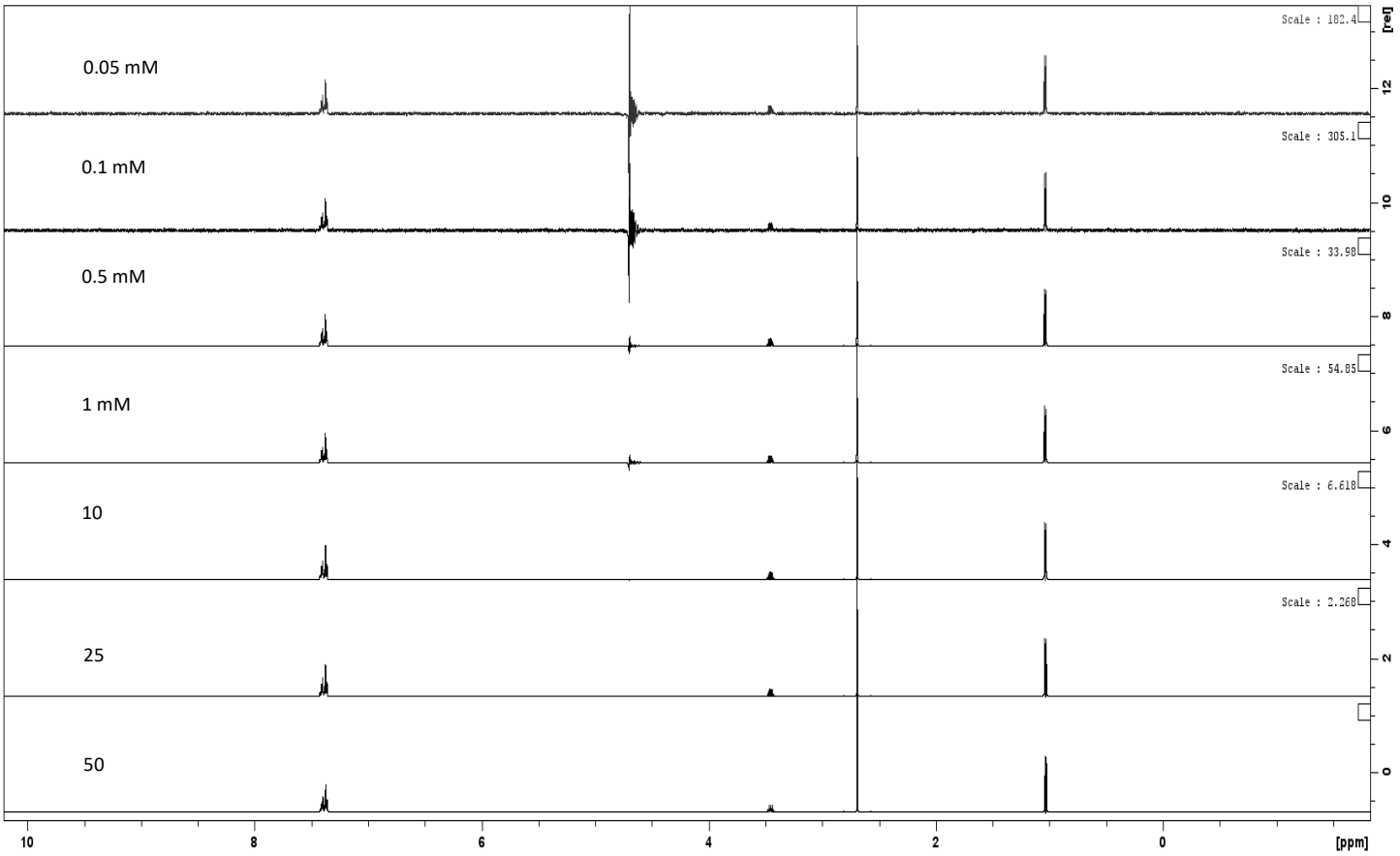

Figure S8. ^{1}H NMR (600 MHz, 298 K) spectra of 0.05 to 50 mM pseudoephedrine $\mathbf{3}^{+}$ in 30 mM phosphate buffer solution at pH 7.0 ± 0.1.

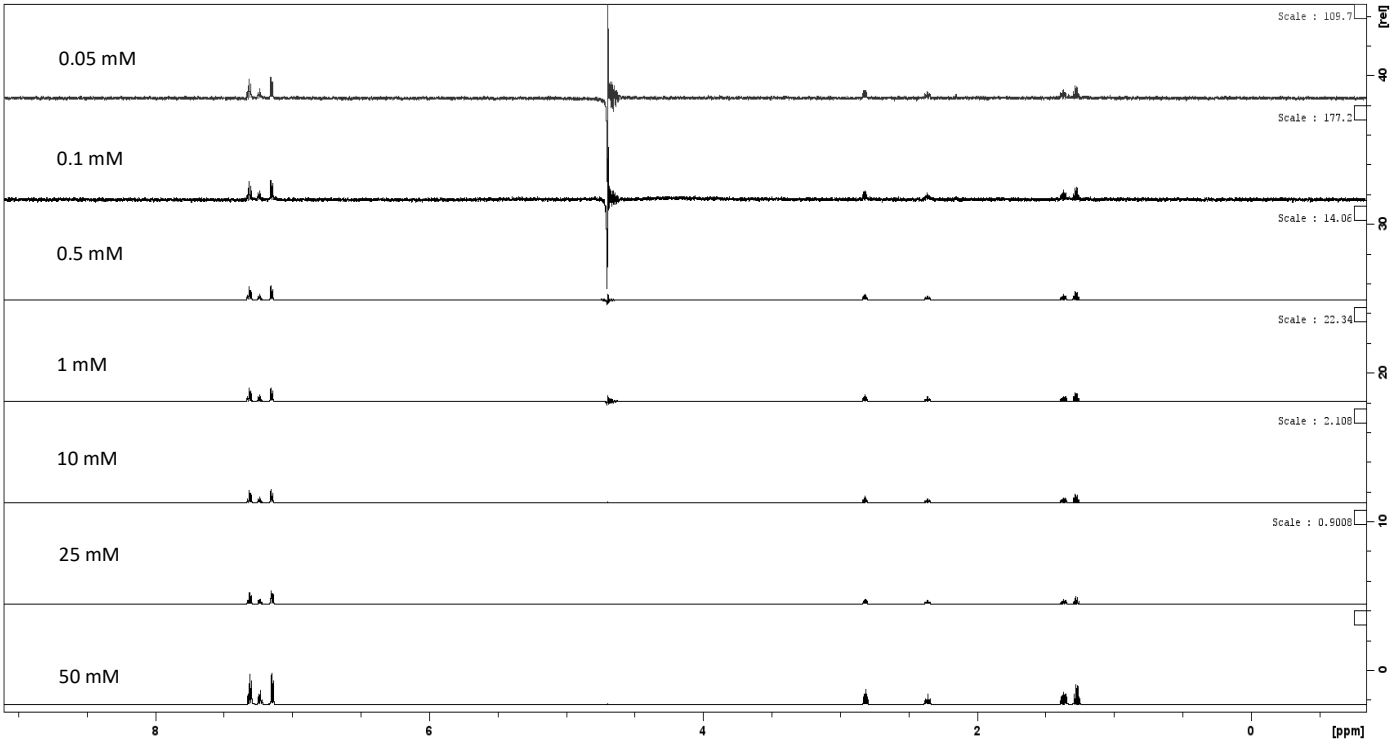

Figure S9. ^{1}H NMR (600 MHz, 298 K) spectra of 0.05 to 50 mM tranylcypromine $\mathbf{4}^{+}$ in 30 mM phosphate buffer solution at pH 7.0 ± 0.1.

Table S1. Akaike information criterion (AIC) scores and Akaike weights (w_i) obtained for three independent titrations in which ephedrine $\mathbf{2}^+$ was added to basket $\mathbf{1}^{6-}$ (Figures S1 and S4). The data were fit to three models (1:1, 1:2, and 2:1) with AIC and w_i obtained using formulas from reference 24.

		Model 1:1	Model 1:2	Model 2:1
AIC	Titration I	-1138.3305	<u>-1240.0953</u>	-1189.5626
w_i		$6 \cdot 10^{-45}$	<u>1</u>	$1 \cdot 10^{-22}$
AIC	Titration II	-1295.6355	<u>-1468.7606</u>	-1425.5940
w_i		$7 \cdot 10^{-76}$	<u>1</u>	$2 \cdot 10^{-19}$
AIC	Titration III	-1116.1261	-1226.2845	<u>-1257.0181</u>
w_i		$7 \cdot 10^{-62}$	$4 \cdot 10^{-14}$	<u>1</u>

Table S2. Akaike information criterion (AIC) scores and Akaike weights (w_i) obtained for three independent titrations in which tranylcypromine $\mathbf{4}^+$ was added to basket $\mathbf{1}^{6-}$ (Figures S3 and S6). The data were fit to three models (1:1, 1:2, and 2:1) with AIC and w_i obtained using formulas from reference 24.

		Model 1:1	Model 1:2	Model 2:1
AIC	Titration I	-975.0808	-1128.6096	<u>-1172.4171</u>
w_i		$2 \cdot 10^{-86}$	$9 \cdot 10^{-20}$	<u>1</u>
AIC	Titration II	-1036.4028	<u>-1301.9258</u>	-1153.9447
w_i		$5 \cdot 10^{-116}$	<u>1</u>	$5 \cdot 10^{-65}$
AIC	Titration III	-1005.8523	<u>-1217.9896</u>	-1154.3860
w_i		$8 \cdot 10^{-93}$	<u>1</u>	$2 \cdot 10^{-28}$

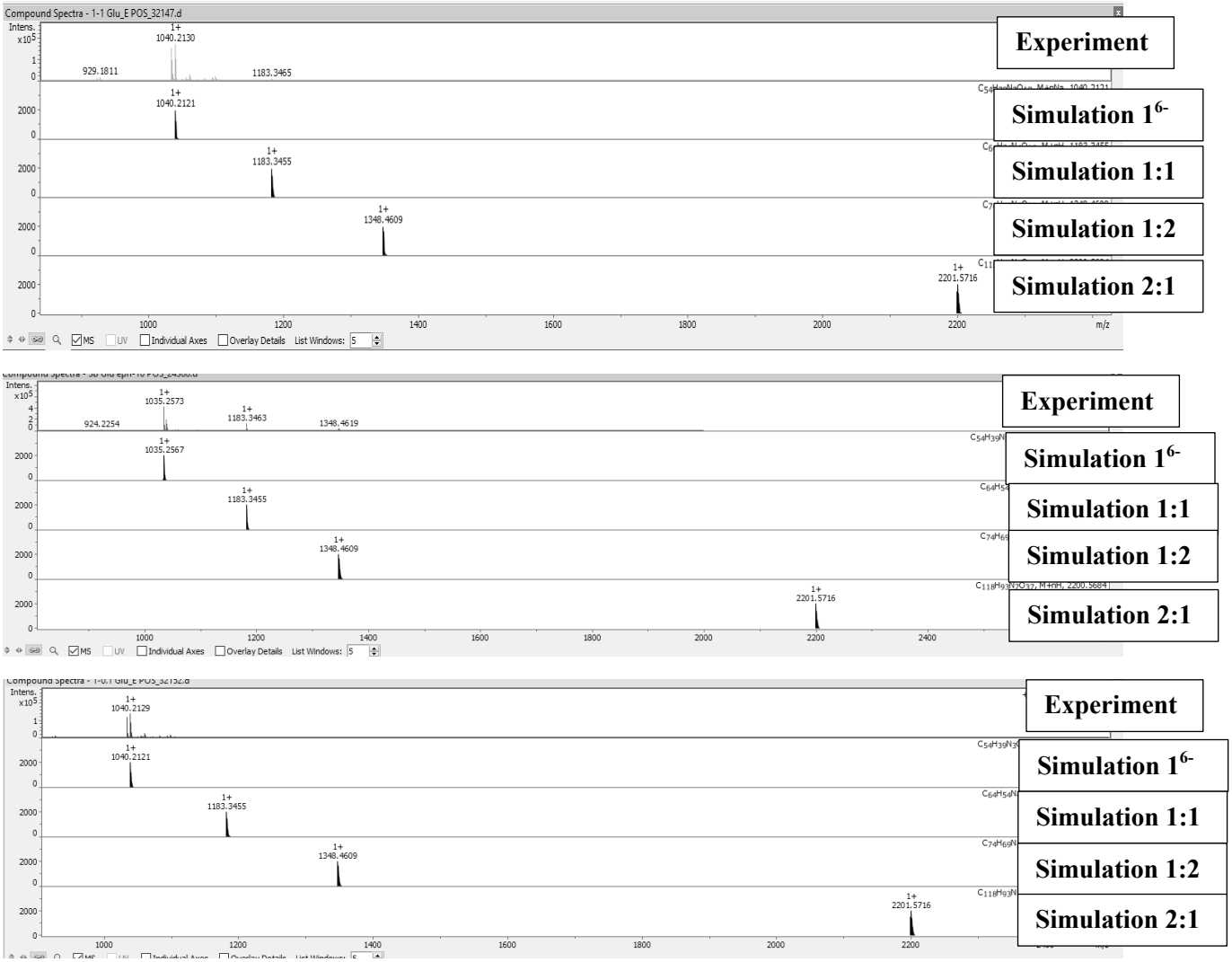

Figure S10. High resolution mass spectra (HRMS – ESI) of three solutions (25mM ammonium bicarbonate buffer at pH 7.0 ± 0.1) of ephedrine $\mathbf{2}^{+}$ and basket $\mathbf{1}^{6-}$ in various proportions: Top – 100 μM of $\mathbf{1}^{6-}$ and 100 μM of ephedrine ($\mathbf{2}^{+}$: $\mathbf{1}^{6-}$ = 1:1); Middle – 10 μM of $\mathbf{1}^{6-}$ and 100 μM of ephedrine ($\mathbf{2}^{+}$: $\mathbf{1}^{6-}$ = 10:1); 100 μM of $\mathbf{1}^{6-}$ and 10 μM of ephedrine ($\mathbf{2}^{+}$: $\mathbf{1}^{6-}$ = 1:10).

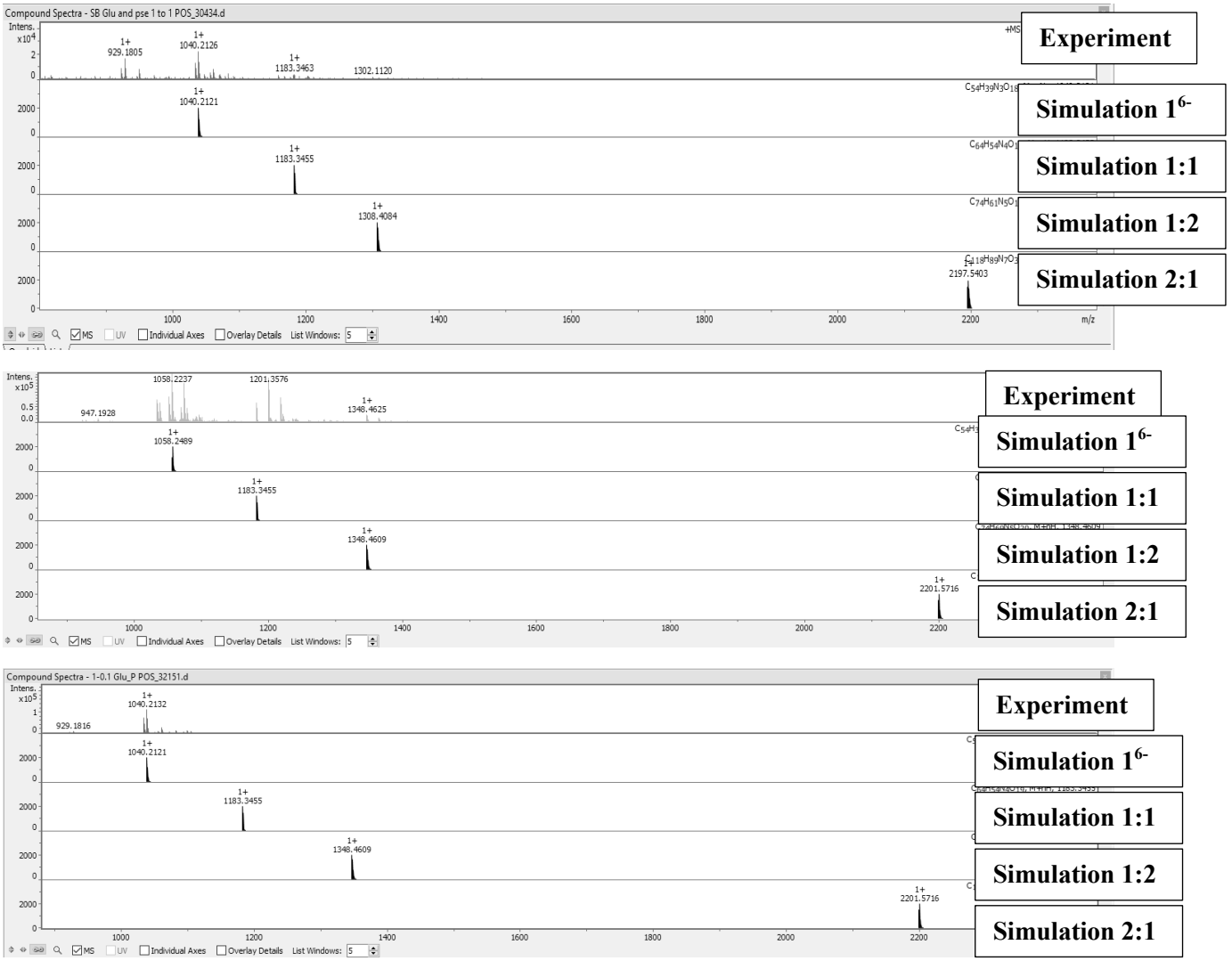

Figure S11. High resolution mass spectra (HRMS – ESI) of three solutions (25mM ammonium bicarbonate buffer at pH 7.0 ± 0.1) of pseudoephedrine $\mathbf{3}^{+}$ and basket $\mathbf{1}^{6-}$ in various proportions: Top – 100 μM of $\mathbf{1}^{6-}$ and 100 μM of pseudoephedrine ($\mathbf{3}^{+}$: $\mathbf{1}^{6-}$ = 1:1); Middle – 10 μM of $\mathbf{1}^{6-}$ and 100 μM of pseudoephedrine ($\mathbf{3}^{+}$: $\mathbf{1}^{6-}$ = 10:1); 100 μM of $\mathbf{1}^{6-}$ and 10 μM of pseudoephedrine ($\mathbf{3}^{+}$: $\mathbf{1}^{6-}$ = 1:10).

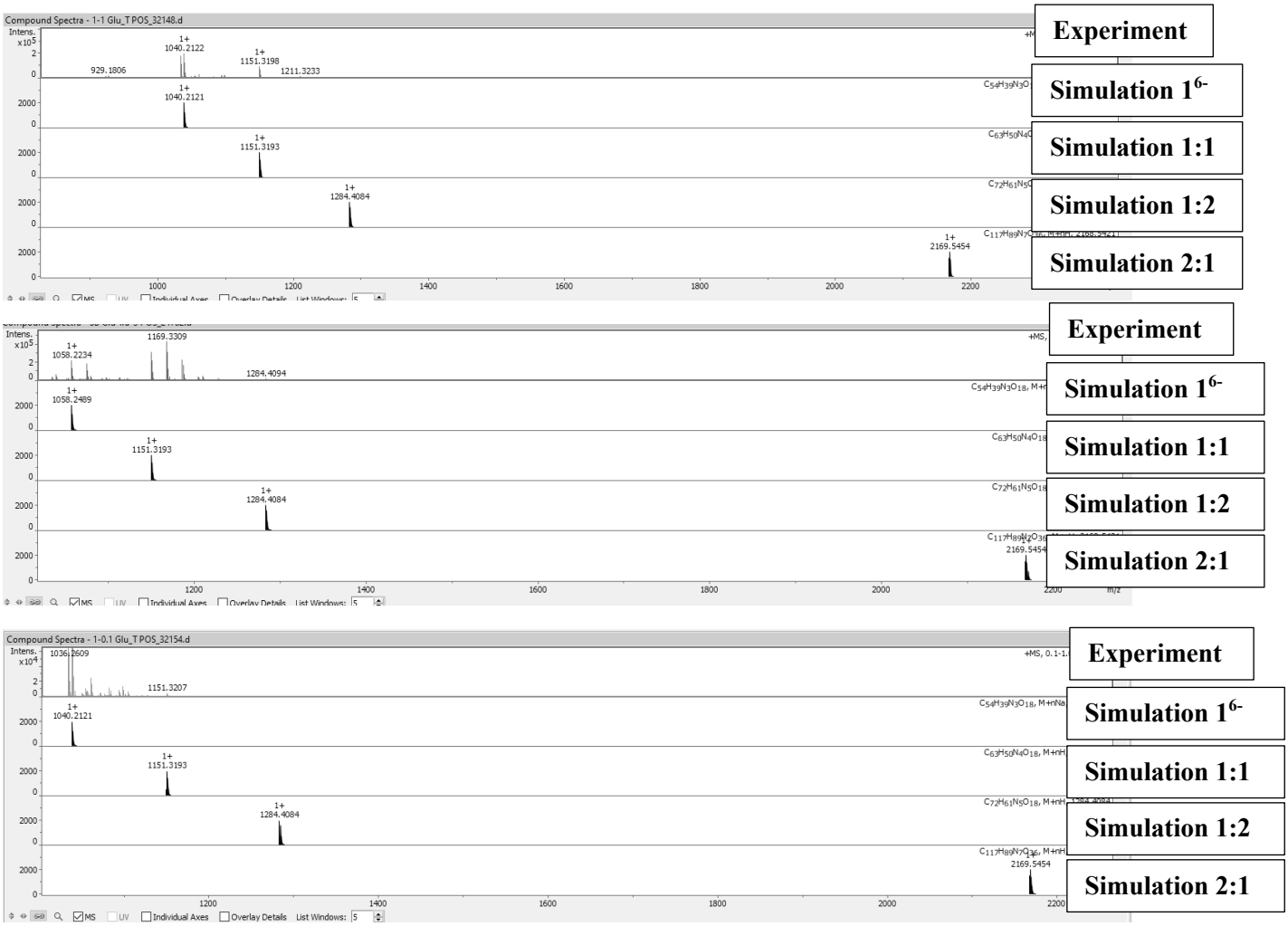

Figure S12. High resolution mass spectra (HRMS – ESI) of three solutions (25mM ammonium bicarbonate buffer at pH 7.0 ± 0.1) of tranylcypromine $\mathbf{4}^{+}$ and basket $\mathbf{1}^{6-}$ in various proportions: Top – 100 μM of $\mathbf{1}^{6-}$ and 100 μM of tranylcypromine ($\mathbf{4}^{+}$: $\mathbf{1}^{6-}$ = 1:1); Middle – 10 μM of $\mathbf{1}^{6-}$ and 100 μM of tranylcypromine ($\mathbf{4}^{+}$: $\mathbf{1}^{6-}$ = 10:1); 100 μM of $\mathbf{1}^{6-}$ and 10 μM of tranylcypromine ($\mathbf{4}^{+}$: $\mathbf{1}^{6-}$ = 1:10).

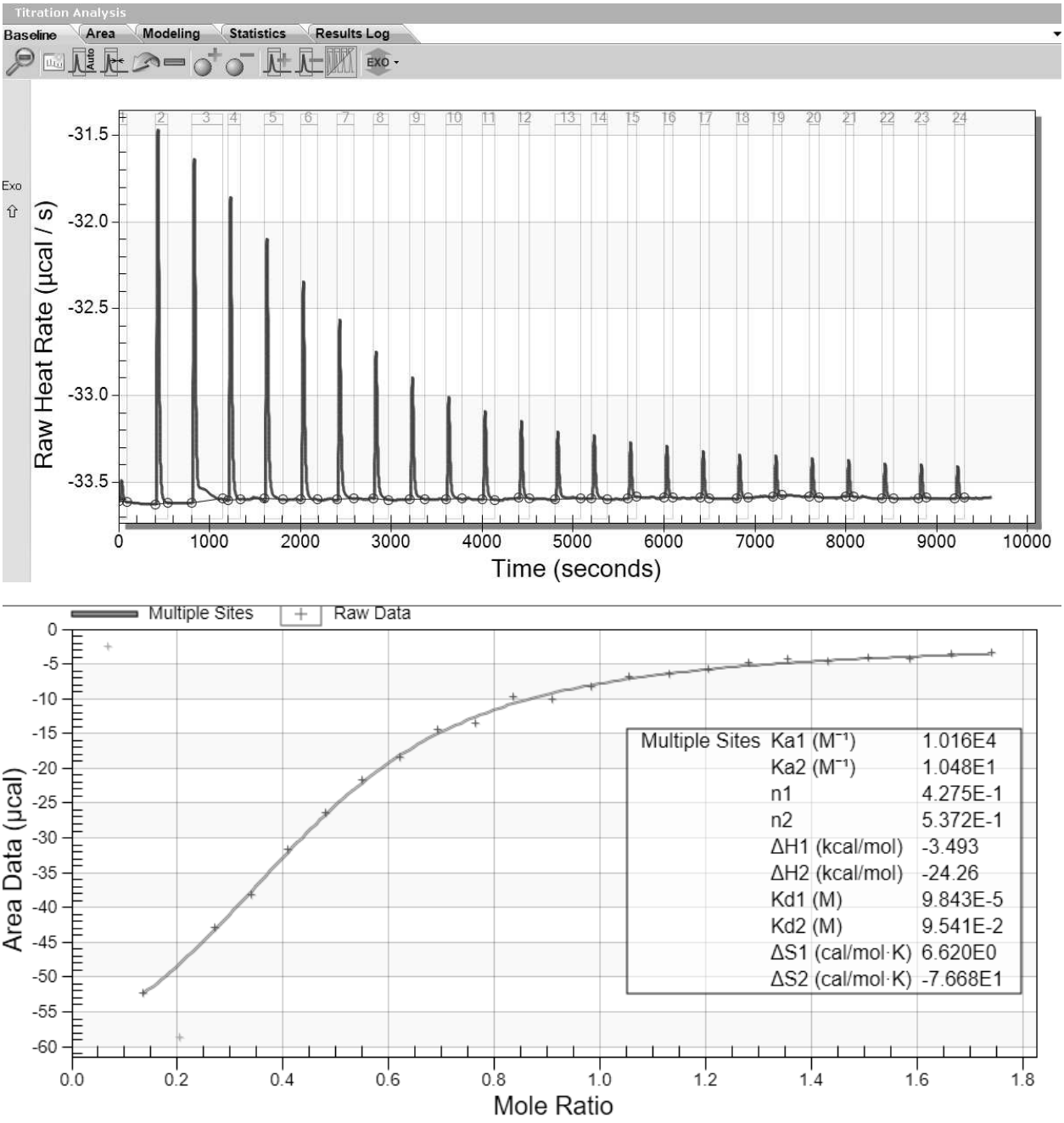

Figure S13. (Top) An incremental addition of 10.0 mM standard solution of tranylcypromine $\mathbf{4}^{+}$ (30 mM aqueous phosphate buffer at pH = 7.0 ± 0.1) to 1.0 mM of basket $\mathbf{1}^{6-}$ (30 mM aqueous phosphate buffer at pH = 7.0 ± 0.1) was monitored with isothermal titration calorimeter (ITC) at 298.0 K. (Bottom) The data were fit to a consecutive binding model (i.e., multiple sites) to give binding constants K_1 and K_2 comparable to those obtained from ^{1}H NMR titration (Figure S6). The data would fit to 1:1 binding model as well although with the n value of circa 0.5. With the assumption that the binding stoichiometry is indeed 1:2 (from ^{1}H NMR and MS measurements), the discrepancy in the n value (and the inflection point) could be due to weak binding and the concentration issues. In any case, the dominant complexation event has $\Delta H^o<0$.

Computational Studies:

General Calculation Notes: To investigate host guest complexes of $\mathbf{1}^{6-}$ with phenethylamines $\mathbf{2}^{+}$–$\mathbf{4}^{+}$, a combination of conformational searches in Schrodinger's Macromodel[1] were used in conjunction with a nucleus independent chemical shift (NICS) calculation carried out in Gaussian 16.[2] All geometry optimizations, completed prior to NICS calculations for the two lowest energy conformers of the host, were completed at the B3LYP/6-31+G(d) level of theory with PCM water solvation. Frequency calculations were carried out for all optimized molecules, to confirm the structures were minima on the potential energy surface. In the following sections the NICS calculation is described, then the concept of combining the calculation of a NICS map with a docking calculation, followed by a more technical explanation of exactly how the two were combined for this study.

Conformational Study of $\mathbf{1}^{6-}$: In order to investigate the conformations of $\mathbf{1}^{6-}$ a conformational search was carried out in Macromodel. For this search the host alone was built in a conformation with all three alpha carboxylates pointing toward the cavity (OPLS3 force field). The search was set up using the Monte Carlo Multiple Minimum (MCMM) method with water solvation. The number of steps was adjusted to 10000, and all other parameters were left at the default settings. Analysis of the conformations produced showed two main poses of the host (each corresponding to a group of conformers with close energy). The first pose was the lowest in energy and was referred to as $\mathbf{1}^{6-}_{A}$ and the second pose was higher in energy and was referred to as $\mathbf{1}^{6-}_{B}$. The structural feature that sets the two poses (sets of conformers) apart is the number of alpha carboxylates they direct toward the center of the host. Specifically, the $\mathbf{1}^{6-}_{A}$ conformer was noted to insert all three alpha carboxylates into the center of the cavity while $\mathbf{1}^{6-}_{B}$ had two alpha carboxylates and one gamma carboxylate pointed towards the center of the cavity. A table is given below which summarizes the energies of the conformers found as well as a designation, A or B, corresponding to the orientation of the glutamate carboxylates (Table S3). Since conformers $\mathbf{1}^{6-}_{A}$ and $\mathbf{1}^{6-}_{B}$ were the most found and were lower in energy, they were selected as representative conformers of the host and used in the following calculations.

Table S3. Energies of conformers found in the MCMM (OPLS3) conformation search for $\mathbf{1}^{6-}$ with designations of A or B for each conformer, $\mathbf{1}^{6-}_{A}$ and $\mathbf{1}^{6-}_{B}$. Additionally, designations of C and D were given for two or three beta carboxylates pointed toward the cavity, respectively.

Conformer Number	OPLS3e Energy (kJ/mol)	Relative Energy (kcal/mol)	Designation
1	-1353.80	0.00	A
2	-1353.50	0.07	A
3	-1350.09	0.89	B
4	-1349.79	0.96	B
5	-1349.22	1.10	B
6	-1346.73	1.69	A
7	-1346.43	1.76	A
8	-1346.43	1.76	A
9	-1346.36	1.78	C
10	-1346.05	1.85	C
11	-1344.32	2.27	B
12	-1343.11	2.56	B
13	-1343.11	2.56	B
14	-1343.04	2.57	D
15	-1342.80	2.63	B
16	-1342.79	2.63	B
17	-1341.50	2.94	A
18	-1341.20	3.01	A
19	-1341.20	3.01	A
20	-1340.55	3.17	C
21	-1339.70	3.37	A
22	-1339.51	3.42	C
23	-1339.38	3.45	A
24	-1339.14	3.51	C
25	-1338.83	3.58	C
26	-1337.82	3.82	B
27	-1337.76	3.83	B
28	-1337.59	3.88	B
29	-1337.54	3.89	B
30	-1337.23	3.96	B
31	-1337.05	4.00	B
32	-1336.80	4.06	B
33	-1336.16	4.22	B
34	-1335.16	4.46	D
35	-1335.10	4.47	B
36	-1334.79	4.54	B
37	-1334.62	4.59	C
38	-1334.43	4.63	A
39	-1334.40	4.64	A
40	-1334.13	4.70	A
41	-1334.04	4.72	C
42	-1333.39	4.88	C

NICS Calculations: A NICS calculation was carried out by calculating magnetic shielding values for a box of ghost atoms with lengths 20 Å x 20 Å x 15 Å centered on the bottom of the host and a 0.1 Å distance between of ghost atoms. The two conformers of basket, $\mathbf{1}^{6\text{-}}{}_{A}$ and $\mathbf{1}^{6\text{-}}{}_{B}$, had NICS maps calculated. To generate the ghost atom coordinates, a MATLAB[3] script was written which can determine a Z axis via the selection of 3 co-planar atoms at the bottom of the host. A grid was then created aligned with the Z axis of the host to form the map. Magnetic shielding values were computed at each of the ghost atom coordinates with B3LYP/6-31+G(d) level of theory with PCM water solvation using the GIAO method.[4-5] The resulting data were analyzed and plotted using MATLAB resulting in shielding maps of the two hosts (Figure S14 and S15).

Magnetic Perturbation of Nuclei - Concept: In NMR titrations for host-guest complexes, one generally observes a steady shift in the chemical shift of resonances corresponding to the host or guest which are then fit to complexation equilibria models to obtain binding constants. Intrinsic to this process is the generation of a parameter, $\Delta\delta$, which describes the change in chemical shift between the bound and free guest:

$$\Delta\delta = \delta_{bound} - \delta_{free}$$

Contributing to the observed chemical shift can be many equilibria. For instance, the δ_{free} state is the Boltzmann weighted average of the chemical shifts of all exchanging conformations of the molecule in solution. The bound state's chemical shift, δ_{bound}, is likewise comprised of the Boltzmann weighted average of the chemical shifts of all exchanging conformations of the host-guest complex. To compute the experimentally observable parameter $\Delta\delta$, the combination of two calculations was used: a Monte-Carlo Molecular Mechanics (MCMM) search with the host frozen (docking) and the previously explained NICS calculation. In this workflow, the NICS calculation provides a map which estimates the "shielding" effect which is typically considered the main contribution to the change in chemical shift upon binding, $\Delta\delta$. With this map, one can take docked poses of the guest molecule in the host and assign a shielding value to each proton based on the closest surrounding points in the NICS map (< 0.1 Å). After each proton in each pose has been assigned an estimate of the $\Delta\delta$ value, one can calculate the ensemble average of all docked poses by weighing the estimated $\Delta\delta$ values by the energies found in the MCMM conformational search. After Boltzmann weighting the contributions to the ensemble average one can then compare the assigned estimates to the observed $\Delta\delta$ values (e.g., Figure 4 in the main text). As described in the main text, we also used an RMSE criterium to identify single pose which best reflects the host-guest complex.

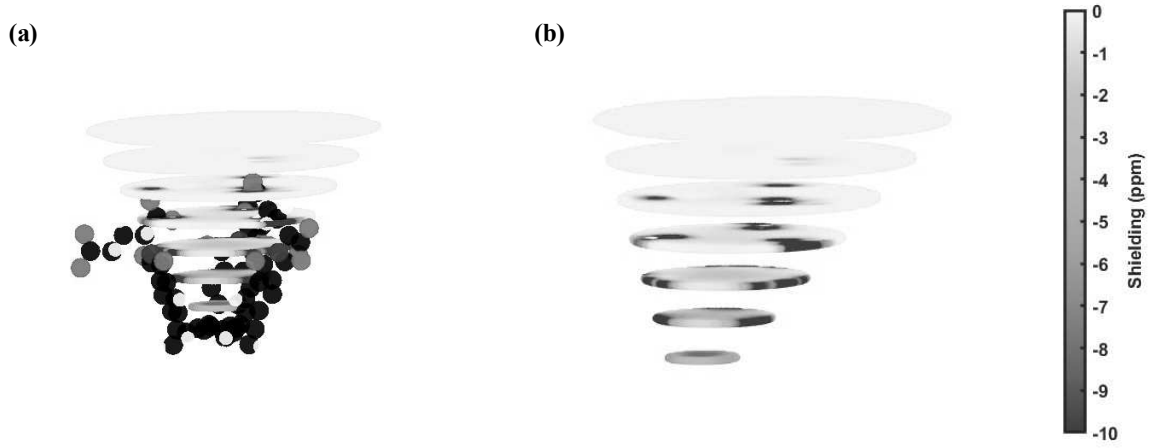

Figure S14. Depictions of the shielding environment for $\mathbf{1}^{6-}_{A}$ (a) with host atoms shown (b) without host atoms shown.

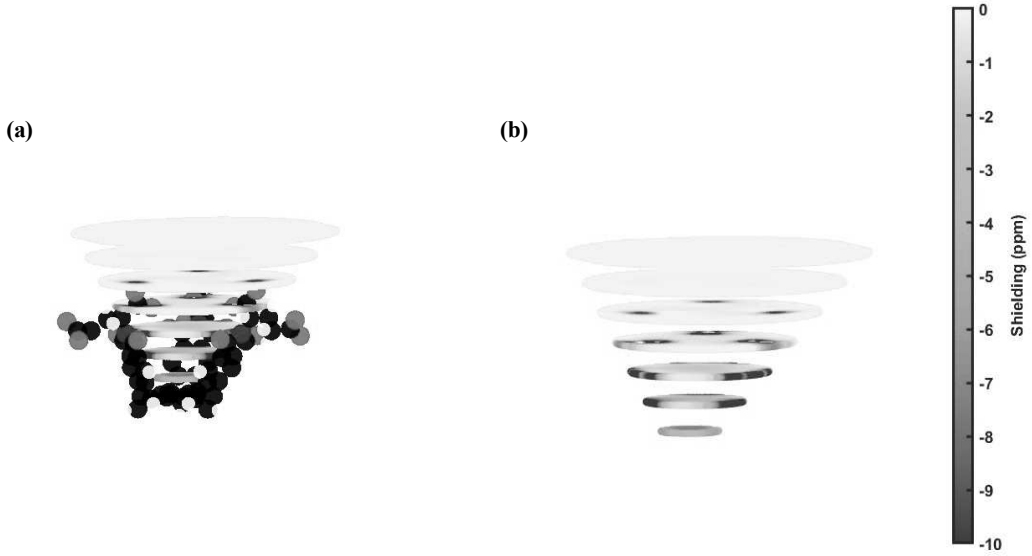

Figure S15. Depictions of the shielding environment for $\mathbf{1}^{6-}_{B}$ (a) with host atoms shown (b) without host atoms shown.

Magnetic Perturbation of Nuclei – Computational Procedure: After generation of the NICS maps for the two hosts, a MCMM search was carried out for [**2**-**4**⊂**1**$_{A/B}$]$^{5-}$ complexes using MacroModel (OPLS3e, water solvation). The MCMM search was prepared such that coordinates of **1**$^{6-}{}_{A}$ and **1**$^{6-}{}_{B}$ basket hosts were frozen while guests **2**$^{+}$-**4**$^{+}$ were allowed to freely move, rotate, and go through dihedral changes within the pocket of the host. This was done by performing manual set-up for the MCMM search (OPLS3) within the MacroModel GUI as explained in MacroModel's manual.[6] From this calculation, essentially docking, many poses were generated for each host-guest pair. Importantly, the hosts' coordinates were fixed in the same position as for the previous NICS calculation to allow the direct comparison of the coordinates of the hydrogens on the guest molecule to the coordinates of ghost atoms in the NICS map. By using a distance criterium, ghost atom coordinates within 0.1 Å of each proton were found and the average of all points within that distance was assigned to that proton as its $\Delta\delta_{comp}$ value. After each pose had all resonances assigned $\Delta\delta_{comp}$ values, the ensemble average <$\Delta\delta_{comp}$> for each resonance was computed by Boltzmann weighting $\Delta\delta_{comp}$ from each pose using its steric energy (see Tables S4-S9):

$$\langle \Delta\delta_{H_i} \rangle = \frac{\sum_{j=1}^{n} \left[e^{-E_j / k_B T} \, \Delta\delta_{(comp)j\,H_i} \right]}{\sum_{j=1}^{n} e^{-E_j / k_B T}}$$

In the formula, $\langle \Delta\delta_{H_i} \rangle$ is the ensemble averaged $\Delta\delta_{comp}$ for proton i, E_j is the energy of pose j, $\Delta\delta_{j,H_i}$ is the assigned $\Delta\delta_{comp}$ for proton i in pose j, and n is equal to the number of poses found in the MCMM search. After calculation of the ensemble averages <$\Delta\delta_{comp}$> for each proton, they were compared with the $\Delta\delta_{exp}$ values from the NMR titrations. Calculated <$\Delta\delta_{comp}$> against $\Delta\delta_{exp}$ values are shown in Figures S16-S18. As discussed in the main text, we used the following approach to identify the binding pose of drugs within baskets. Each computed pose of [**2**-**4**⊂**1**]$^{5-}$ had assigned $\Delta\delta_{comp}$ value for each proton from **2**$^{+}$-**4**$^{+}$. For each pose, we then compared these values to $\Delta\delta_{exp}$ values using an RMSE method:

$$RMSE = \sqrt{\frac{1}{N} \sum_{i=1}^{N} \left(\Delta\delta_{comp,i} - \Delta\delta_{exp,i} \right)^2}$$

Where above N is the number of observable protons in each guest molecule. After RMSE analysis, the pose with the lowest RMSE was taken as the representative structure for the host guest complex (Figures S19-S21).

Table S4. Energies of conformers found in the MCMM (OPLS3) conformation search for $\mathbf{1}^{6-}_{A}$ with ephedrine $\mathbf{2}^{+}$.

Conformer	Energy OPLS3e (kJ/mol)	Conformer	Energy OPLS3e (kJ/mol)
1	-3888.857	20	-3873.081
2	-3888.208	21	-3873.057
3	-3887.955	22	-3872.558
4	-3884.369	23	-3872.304
5	-3884.018	24	-3871.888
6	-3883.788	25	-3871.693
7	-3883.119	26	-3871.668
8	-3879.516	27	-3871.271
9	-3878.947	28	-3871.161
10	-3878.539	29	-3870.798
11	-3877.853	30	-3870.745
12	-3876.667	31	-3870.695
13	-3874.891	32	-3870.512
14	-3874.658	33	-3869.733
15	-3874.317	34	-3869.343
16	-3874.199	35	-3869.299
17	-3873.881	36	-3869.104
18	-3873.393	37	-3868.459
19	-3873.16	38	-3868.378

Table S5. Energies of conformers found in the MCMM conformation search (OPLS3) for $\mathbf{1}^{6-}_{A}$ with pseudoephedrine $\mathbf{3}^{+}$.

Conformer	Energy OPLS3e (kJ/mol)	Conformer	Energy OPLS3e (kJ/mol)
1	-3873.083	27	-3858.165
2	-3871.267	28	-3857.601
3	-3871.021	29	-3857.291
4	-3869.941	30	-3856.864
5	-3869.915	31	-3856.271
6	-3869.092	32	-3855.425
7	-3868.764	33	-3855.232
8	-3868.542	34	-3855.147
9	-3868.397	35	-3854.886
10	-3865.416	36	-3854.801
11	-3864.906	37	-3854.665
12	-3864.271	38	-3854.593
13	-3864.167	39	-3854.517
14	-3863.66	40	-3854.374
15	-3862.932	41	-3853.993
16	-3861.849	42	-3853.941
17	-3860.684	43	-3853.939
18	-3860.664	44	-3853.599
19	-3860.18	45	-3853.38
20	-3860.08	46	-3853.205
21	-3859.446	47	-3852.976
22	-3859.201	48	-3852.796
23	-3859.02	49	-3852.736
24	-3858.641	50	-3852.685
25	-3858.455	51	-3852.528
26	-3858.219	52	-3852.36
		53	-3852.128

Table S6. Energies of conformers found in the MCMM conformation search (OPLS3) for $\mathbf{1}^{6-}_{A}$ with tranylcypromine $\mathbf{4}^{+}$.

Conformer	Energy OPLS3e (kJ/mol)
1	-3902.989
2	-3902.941
3	-3902.65
4	-3902.208
5	-3901.936
6	-3901.524
7	-3900.746
8	-3899.852
9	-3899.317
10	-3898.197
11	-3893.906
12	-3892.924
13	-3890.053
14	-3889.979
15	-3889.114

Table S7. Energies of conformers found in the MCMM conformation search (OPLS3) for $\mathbf{1}^{6-}{}_{B}$ with ephedrine $\mathbf{2}^{+}$.

Conformer	Energy OPLS3e (kJ/mol)
1	-3985.49
2	-3983.412
3	-3982.227
4	-3975.632
5	-3973.047
6	-3972.781
7	-3971.389
8	-3969.826
9	-3969.351
10	-3968.989
11	-3967.426
12	-3967.164
13	-3966.206
14	-3965.75
15	-3965.117

Table S8. Energies of conformers found in the MCMM conformation search (OPLS3) for $\mathbf{1}^{6-}_{B}$ with pseudoephedrine $\mathbf{3}^{+}$.

Conformer	Energy OPLS3e (kJ/mol)	Conformer	Energy OPLS3e (kJ/mol)
1	-3967.762	24	-3953.788
2	-3965.665	25	-3952.553
3	-3965.152	26	-3952.353
4	-3964.09	27	-3952.055
5	-3963.893	28	-3951.892
6	-3963.309	29	-3950.857
7	-3962.989	30	-3950.72
8	-3960.152	31	-3949.885
9	-3960.042	32	-3949.798
10	-3959.121	33	-3949.775
11	-3958.988	34	-3949.719
12	-3957.821	35	-3949.707
13	-3957.534	36	-3949.387
14	-3957.414	37	-3948.869
15	-3956.785	38	-3948.851
16	-3956.646	39	-3948.344
17	-3956.31	40	-3948.079
18	-3956.061	41	-3947.833
19	-3955.825	42	-3947.457
20	-3954.516	43	-3947.254
21	-3954.499	44	-3947.038
22	-3954.259	45	-3946.931
23	-3954.083		

Table S9. Energies of conformers found in the MCMM conformation search (OPLS3) for $\mathbf{1}^{6-}_{B}$ with tranylcypromine $\mathbf{4}^{+}$.

Conformer	Energy OPLS3e (kJ/mol)
1	-4009.645
2	-4005.702
3	-4002.858
4	-4002.211
5	-4001.441
6	-4001.023
7	-3999.733
8	-3997.431
9	-3996.416
10	-3995.733
11	-3993.74
12	-3993.445
13	-3991.671
14	-3990.883
15	-3990.795
16	-3988.729

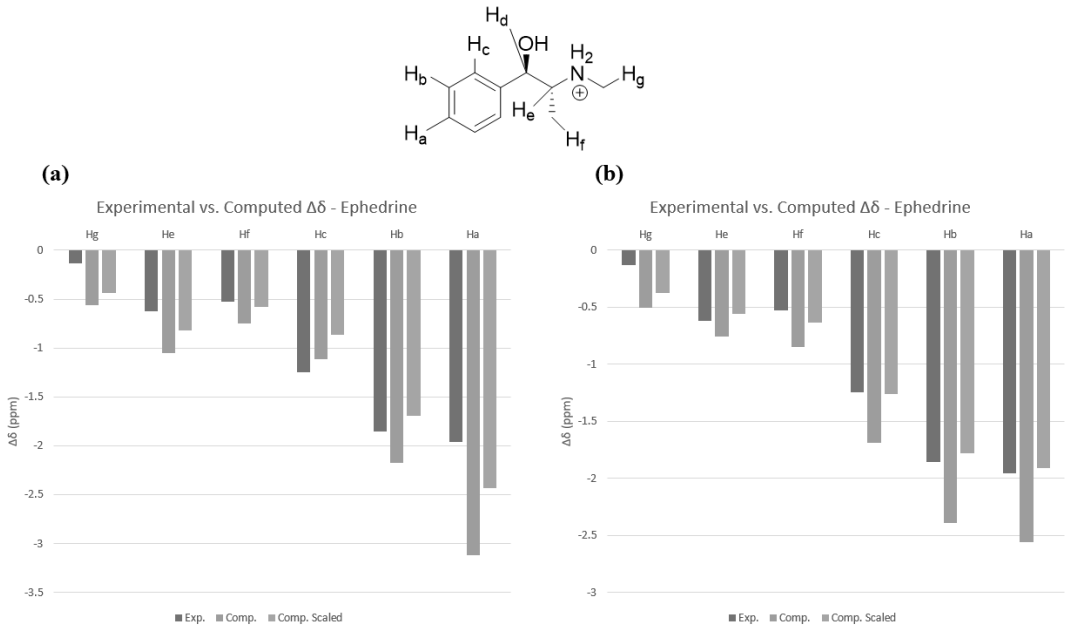

Figure S16. (a) Bar graph showing the ensemble averaged $<\Delta\delta_{comp}>$ and experimental $\Delta\delta_{exp}$ values for ephedrine $\mathbf{2}^{+}$ docked inside basket $\mathbf{1}^{6-}{}_{A}$. (b) Bar graph showing the ensemble averaged $<\Delta\delta_{comp}>$ and experimental $\Delta\delta_{exp}$ for ephedrine $\mathbf{2}^{+}$ docked inside basket $\mathbf{1}^{6-}{}_{B}$.

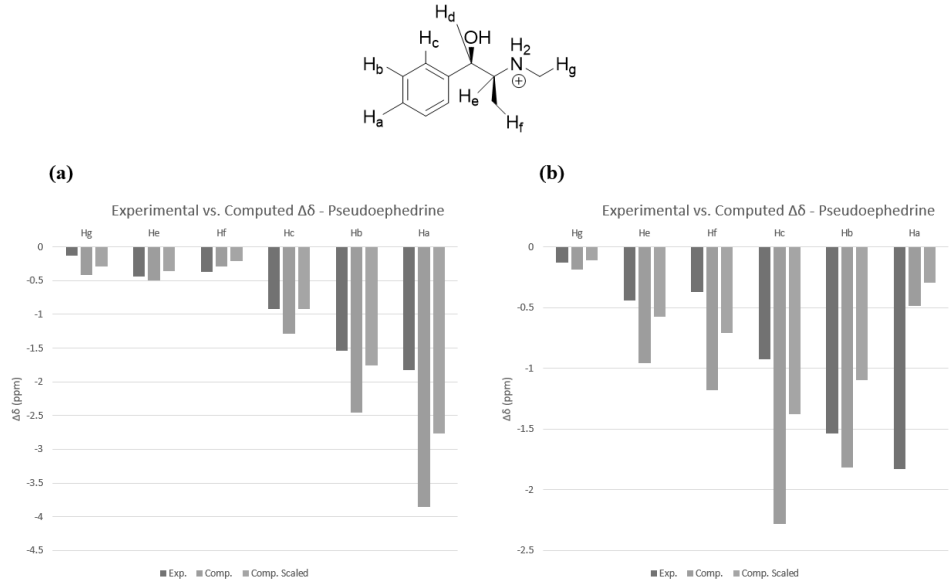

Figure S17. (a) Bar graph showing the ensemble averaged $<\Delta\delta_{comp}>$ and experimental $\Delta\delta_{exp}$ values for pseudoephedrine $\mathbf{3}^{+}$ docked inside basket $\mathbf{1}^{6-}{}_{A}$. (b) Bar graph showing the ensemble averaged $<\Delta\delta_{comp}>$ and experimental $\Delta\delta_{exp}$ values for pseudoephedrine $\mathbf{3}^{+}$ docked inside basket $\mathbf{1}^{6-}{}_{B}$.

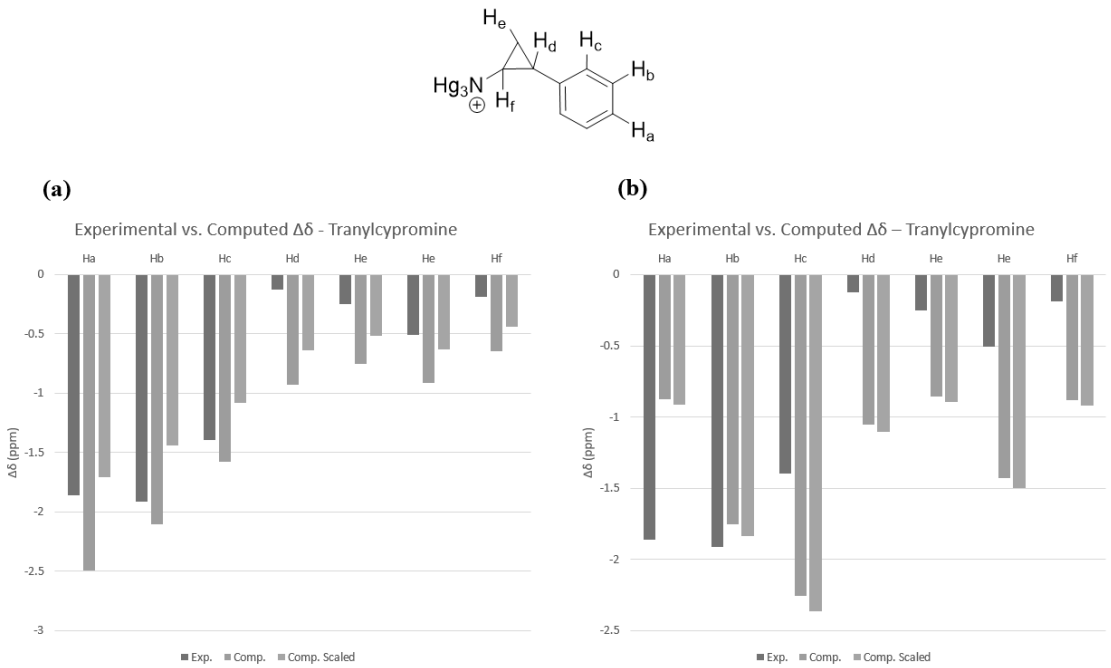

Figure S18. (a) Bar graph showing the ensemble averaged $<\Delta\delta_{comp}>$ and experimental $\Delta\delta_{exp}$ values for tranylcypromine $\mathbf{4}^{+}$ docked inside basket $\mathbf{1}^{6-}{}_{A}$. (b) Bar graph showing the ensemble averaged $<\Delta\delta_{comp}>$ and experimental $\Delta\delta_{exp}$ values for tranylcypromine $\mathbf{4}^{+}$ docked inside basket $\mathbf{1}^{6-}{}_{A}$.

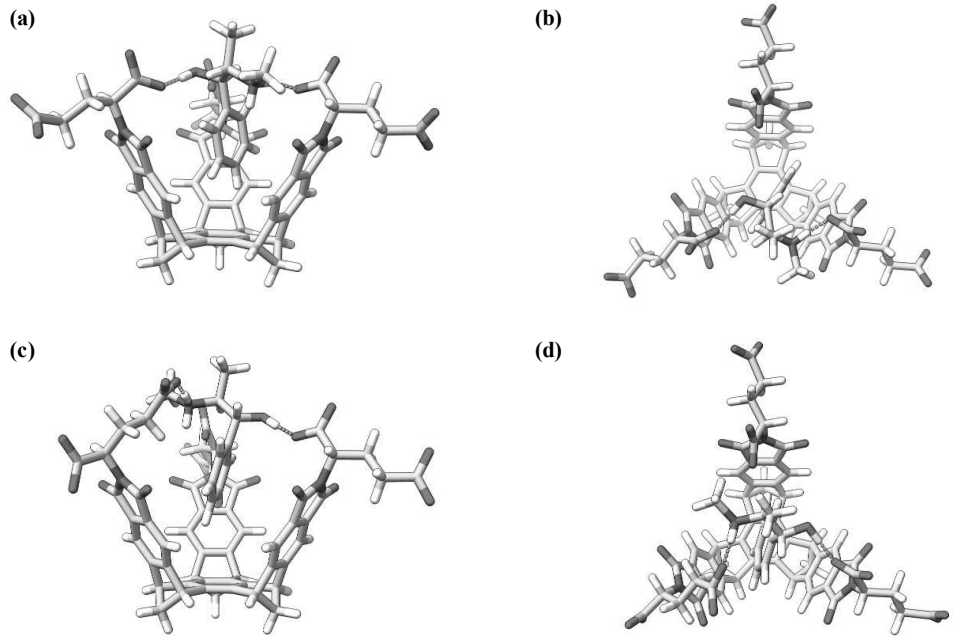

Figure S19. (a/b) Two views of $[\mathbf{2}\subset\mathbf{1}_A]^{5-}$ having the lowest RMSE (Table 3 from main text). (c/d) Two views of $[\mathbf{2}\subset\mathbf{1}_B]^{5-}$ having the lowest RMSE (Table 3 from main text).

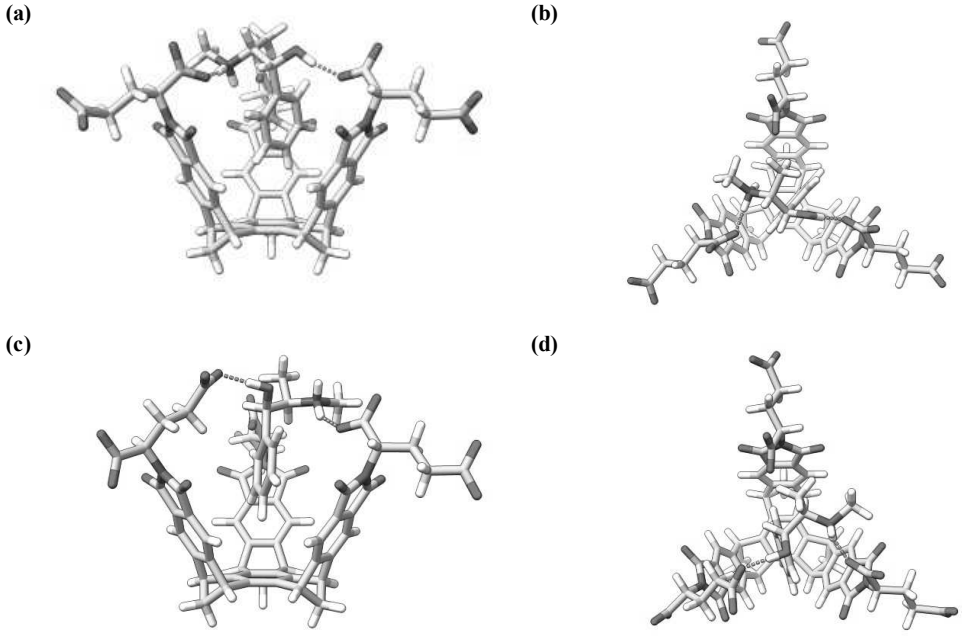

Figure S20. (a/b) Two views of $[\mathbf{3}\subset\mathbf{1}_A]^{5-}$ having the lowest RMSE (Table 3 from main text). (c/d) Two views of $[\mathbf{3}\subset\mathbf{1}_B]^{5-}$ having the lowest RMSE (Table 3 from main text).

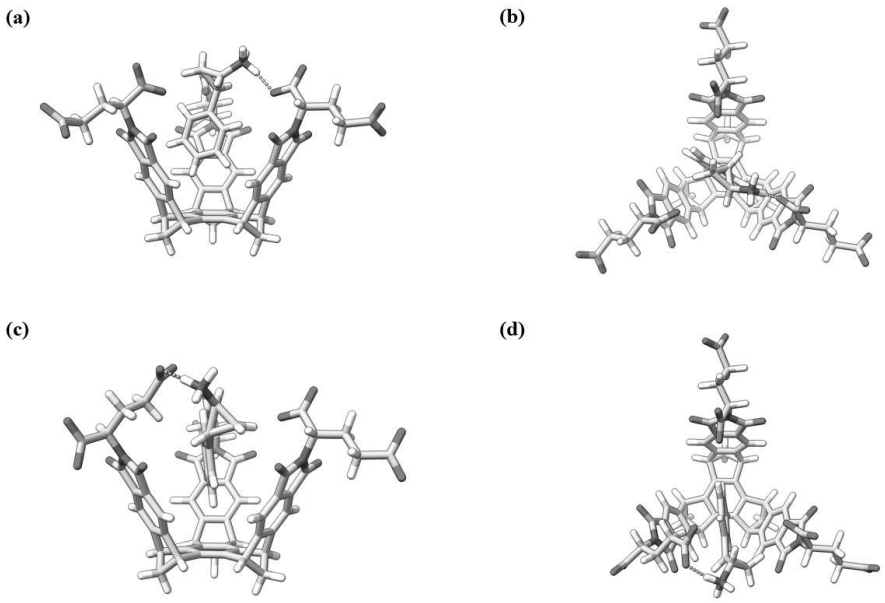

Figure S21. (a/b) Two views of $[\mathbf{4}\subset\mathbf{1}_A]^{5-}$ having the lowest RMSE (Table 3 from main text). (c/d) Two views of $[\mathbf{4}\subset\mathbf{1}_B]^{5-}$ having the lowest RMSE (Table 3 from main text).

Optimized Coordinates from DFT Calculations:

$\mathbf{1}^{6-}_A$

E(RB3LYP) = -3597.146467

Number of Imaginary Frequencies = 0

Cartesian Coordinates:

O 14.79349500 -7.65289700 15.70683800

O 15.07238500 -4.04475700 18.55293400

O 18.10629700 -6.81330000 19.27538200

O 15.88292900 -7.13091700 19.51543300

N 15.30023300 -5.89842100 17.15370800

C 14.45296800 -6.66520700 16.34552400

C 13.10317400 -6.04125500 16.42368300

C 13.18648300 -4.95693700 17.29840500

C 14.59531900 -4.86420700 17.78023900

C 11.91826600 -6.37956000 15.76592800

H 11.86733200 -7.22058600 15.08001500

C 10.82177500 -5.56256300 16.02722100

C 10.90278200 -4.46898900 16.92380100

C 12.08662500 -4.14365800 17.58057300

H 12.16057800 -3.30023600 18.26143900

C 9.38782200 -5.58581000 15.49486300

H 9.23018300 -6.15574400 14.57856500

C 9.12392600 -4.04428100 15.45262400

H 9.78289000 -3.51556000 14.75566300

H 8.07844900 -3.79590900 15.24375000

C 9.51612100 -3.82425600 16.95120300

H 9.47158700 -2.80886200 17.34655700

C 8.49338200 -5.94698100 16.68508200

C 7.68224800 -7.01974300 16.97048800

C 16.69988700 -6.24701800 17.41334100

H 16.88131300 -7.11865800 16.77299600

C 16.90762700 -6.76094800 18.88340600
C 17.67224000 -5.13340500 16.98300600
O 18.37948100 -2.50018400 15.29109200
O 19.73574500 -4.18295800 14.64145700
C 18.64489400 -3.72617000 15.10113800
O 8.50078500 -12.84238000 20.92033600
O 10.87706600 -12.80919700 16.97790700
O 12.38049600 -12.65728100 19.94468000
O 12.93459400 -14.84726800 19.92837600
N 9.85037700 -13.14477600 19.04574600
C 8.86871800 -12.49745300 19.80455600
C 8.38418600 -11.34812700 18.99022600
C 9.11384400 -11.33357200 17.80048400
C 10.06763500 -12.47981000 17.83374400
C 7.37571600 -10.41903700 19.25755500
H 6.80816100 -10.44386800 20.18363700
C 7.13130400 -9.48034100 18.25876700
C 7.87675900 -9.46138700 17.05457500
C 8.88737400 -10.38471900 16.80111900
H 9.45811100 -10.38236500 15.87665600
C 6.11528800 -8.34044200 18.16123500
H 5.26999800 -8.39726400 18.84786600
C 5.81868100 -8.41689800 16.62694400
H 5.36164600 -9.36547900 16.32554800
H 5.21564900 -7.57739800 16.26649700
C 7.32487900 -8.30665300 16.21794600
H 7.56820600 -8.33113900 15.15517800
C 6.92429000 -7.03907400 18.18119800
C 7.00165800 -5.98254500 19.05759900
C 10.63298700 -14.28291600 19.53569000
H 10.20480800 -14.49787200 20.52229800
C 12.12806300 -13.88385200 19.80866100
C 10.45620500 -15.53470900 18.65681600
H 11.06430500 -16.32201700 19.11181300
H 10.86628400 -15.34704100 17.65883200
O 8.87618200 -17.17345000 16.44065100
O 8.87124600 -18.40455700 18.33217000
C 8.99592200 -16.01046700 18.53901400
H 8.58950300 -16.19272800 19.54152700
H 8.38921700 -15.23133500 18.06165200
C 8.89752600 -17.30348600 17.70246200
O 11.49096600 -4.15042200 24.24033500
O 8.76616400 -7.74010200 25.18182700
O 12.08104100 -8.04091400 24.80107900
O 12.47268500 -8.12013200 27.02450900
N 10.30291700 -5.98957700 25.03649700
C 10.57468700 -4.95563500 24.13324300
C 9.54347800 -5.03854300 23.06168000
C 8.72010700 -6.12825500 23.34866900
C 9.21453200 -6.75774900 24.60706600
C 9.32876300 -4.21333000 21.95513000
H 9.97269200 -3.36411400 21.74402400
C 8.23115000 -4.53270800 21.16033500
C 7.39458000 -5.63756100 21.45298300
C 7.62556500 -6.46426700 22.54911900
H 6.98608700 -7.31039900 22.78469800
C 7.65506600 -3.86868500 19.90817800
H 7.98231500 -2.84556200 19.71990600
C 6.13515400 -4.11075200 20.19078700
H 5.78134300 -3.60344600 21.09466300
H 5.49628500 -3.85287100 19.34008500
C 6.30352900 -5.65464500 20.38190300
H 5.41409400 -6.23938200 20.61926600
C 7.84389000 -4.86718600 18.76052700
C 8.57547800 -4.84933700 17.59621900
C 11.14814400 -6.29526500 26.19430000
H 11.89879900 -5.49572100 26.19768000
C 11.95958800 -7.62398500 25.98350600

C 10.36771400 -6.22203900 27.51957300

H 11.07707900 -6.47093000 28.31408500

H 9.58779300 -6.99091800 27.52986700

O 7.78736800 -5.21446600 29.13900900

O 9.64505500 -4.44864200 30.16649600

C 9.74379100 -4.84062900 27.79487600

H 10.53551600 -4.08091000 27.80834900

H 9.03946300 -4.58518000 26.99412300

C 8.99475700 -4.82471200 29.14424100

H 18.67994200 -5.50391400 17.19182700

H 17.51873300 -4.24612300 17.60652600

C 17.56105900 -4.75248400 15.49430500

H 16.57091600 -4.32672600 15.29169800

H 17.67720500 -5.65380300 14.87949600

1^{6-}_{B}

E(RB3LYP) = -3597.145754

Number of Imaginary Frequencies = 0

Cartesian Coordinates:

C -5.46942500 -10.58765400 -1.39060700

C -5.03841200 -10.62807300 -2.69575100

C -3.67404900 -10.93560000 -2.98768200

C -4.55394200 -10.85687300 -0.32701800

C -5.36648600 -10.77920800 0.97027000

C -6.71755500 -11.36849700 0.44524300

H -4.91793700 -11.23849500 1.85184800

C -6.83278100 -10.34587300 -0.73350500

H -7.53373000 -11.28036300 1.17025700

H -6.62760000 -12.40482900 0.10416300

H -7.70437000 -10.41474600 -1.38530000

C -6.70235400 -9.05073200 0.07030100

C -5.79560800 -9.31944000 1.12493900

C -7.30298700 -7.80391900 -0.08067600

C -5.45714000 -8.35187500 2.06703100

C -6.97115900 -6.84510200 0.87990700

H -8.00416400 -7.58905000 -0.88233600

C -6.07903300 -7.11005900 1.91921300

H -4.76801700 -8.55092800 2.88306000

C -3.24179200 -11.15660600 -0.60841100

C -2.79402800 -11.19819900 -1.96453300

C -2.03514300 -11.54188300 0.25472000

H -2.24963500 -11.84806100 1.27919800

C -1.31902600 -11.61192800 -1.91856100

H -0.88970900 -11.98130600 -2.85055800

C -1.38137200 -12.59380000 -0.70169500

H -0.39213000 -12.92216300 -0.36533900

H -2.02348200 -13.46121000 -0.88521600

C -1.01001600 -10.41731000 0.09600000

C -0.51073600 -9.48583300 1.00245700

C -0.56680900 -10.46158000 -1.24850800

C 0.46138400 -8.61225400 0.50884000

H -0.83862600 -9.44814500 2.03758300

C 0.39199300 -9.57738500 -1.73555400

C 0.89843800 -8.65679000 -0.81568300

H 0.74358600 -9.60909400 -2.76309900

C -5.73809000 -10.44886000 -4.04812700

H -6.82720600 -10.50441300 -4.04207700

C -3.55017600 -10.93405200 -4.51505100

H -2.66970400 -11.42479700 -4.93125800

C -4.95464300 -11.52416400 -4.87154500

H -5.17564300 -11.48700200 -5.94360300

H -5.09891100 -12.54103300 -4.49269800

C -5.13835900 -9.19214400 -4.67979100

C -5.69705000 -7.95298800 -4.98045200

C -3.78327600 -9.49010800 -4.96473100

C -4.84334900 -7.02773300 -5.58469800

H -6.73770300 -7.71860500 -4.77414600
C -2.93474700 -8.55552600 -5.55222800
C -3.50613300 -7.31784700 -5.85815600
H -1.89453500 -8.77468000 -5.77653500
C 1.23469200 -7.54575200 1.20435100
C 1.95952700 -7.62194800 -0.98350600
C -7.46364800 -5.45077600 1.05281300
C -5.98947900 -5.88816500 2.77045000
C -2.90995900 -6.12157500 -6.51583200
C -5.12316100 -5.64716900 -6.07501100
O -6.18133600 -5.03557800 -6.02297800
O -1.75498400 -5.96248000 -6.89080100
O 2.58690500 -7.35000100 -1.99787200
O 1.13794000 -7.17959000 2.36902700
O -5.32609300 -5.73456700 3.78646600
O -8.28391700 -4.85040300 0.36976500
N -3.93397900 -5.17586800 -6.64255000
N -6.81353200 -4.92425600 2.17605300
N 2.13044700 -7.01871400 0.26743700
C -3.71540300 -3.81523800 -7.14576600
H -2.67512600 -3.82264400 -7.49300200
C -4.61787300 -3.47689200 -8.34710600
H -5.66570300 -3.46954000 -8.03076500
H -4.37336200 -2.45479400 -8.64377300
C -4.43412400 -4.41978300 -9.53931100
H -3.37535700 -4.44261600 -9.83945700
H -4.68106200 -5.45320600 -9.26219900
C 3.01545300 -5.88283600 0.54723200
C 4.49978400 -6.22350100 0.31885400
H 4.67059700 -6.42671900 -0.74468600
H 5.07361800 -5.32850200 0.56571600
C 4.99701600 -7.40239600 1.16488500
H 4.43915900 -8.31570800 0.93076200
H 4.80910000 -7.18848000 2.22936500
C -7.19012500 -3.63843900 2.77528300
H -7.81639100 -3.16077100 2.01277400
C -5.98187700 -2.72085200 3.04178400
H -5.33151200 -3.16789200 3.79809400
H -6.38579300 -1.80217200 3.47591300
C -5.17563600 -2.38529500 1.78371400
H -5.83604300 -1.98138700 1.00436200
H -4.73765400 -3.29868900 1.35495900
C -3.75969100 -2.75712900 -5.98610200
O -3.69841800 -3.18712900 -4.80362100
O -3.79562400 -1.55084900 -6.35740900
C -5.25452700 -4.07579400 -10.80663000
O -5.18338600 -4.91842000 -11.75418300
O -5.91908600 -2.99930500 -10.82701200
C 2.52760200 -4.57855400 -0.17791100
C 6.50837600 -7.70614900 1.02912700
C -4.01208000 -1.38389400 1.98139500
C -8.12538000 -3.83700700 4.02112200
O -8.41292000 -2.77994300 4.64940800
O 3.35016800 -3.62067500 -0.17964900
O 1.35498400 -4.57535900 -0.63783600
O -3.53277800 -0.87610700 0.92138900
O -3.60520500 -1.15440500 3.15806600
O 6.85099300 -8.92750700 1.07958700
O 7.29993100 -6.72417300 0.91294200
O -8.54502800 -5.00106200 4.26028400
H 2.87334100 -5.69053000 1.61768700

References

1. Schrödinger Release 2022-2: MacroModel, Schrödinger, LLC, New York, NY, 2021.

2. Frisch, M.J. et al. Gaussian 16, Revision C.01, Gaussian, Inc., Wallingford CT, 2016.

3. MATLAB. (2010). *version R2021a*. Natick, Massachusetts: The MathWorks Inc.

4. Ditchfield, R. Self-consistent perturbation theory of diamagnetism. Mol. Phys. 1974, 27, 789-807.
5. Wolinski, K.; Hinton, J. F.; Pulay, P. Efficient Implementation of the Gauge-Independent Atomic Orbital Method for NMR Chemical Shift Calculations. J. Am. Chem. Soc. 1990, 112, 8251-8260

6. http://gohom.win/ManualHom/Schrodinger/Schrodinger_2015-2_docs/macromodel/macromodel_user_manual.pdf